Paradoxical Pro-inflammatory Responses by Human Macrophages to an Amoebae Host-Adapted Legionella Effector

Price, Christopher; Jones, Snake; Mihelčić, Mirna; Šantić, Marina; Abu Kwaik, Yousef

Download date / Datum preuzimanja: **2024-12-31**

Paradoxical Pro-inflammatory Responses by Human Macrophages to an Amoebae Host-Adapted *Legionella* Effector

Graphical Abstract
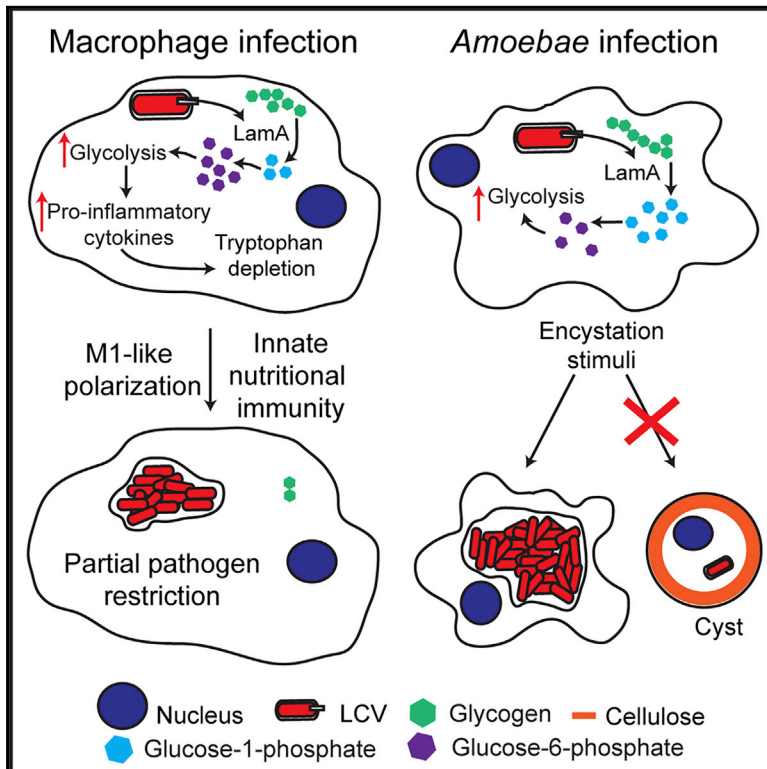
Authors

Christopher Price, Snake Jones,
Mirna Mihelcic, Marina Santic,
Yousef Abu Kwaik

Correspondence

abukwaik@louisville.edu

In Brief

Legionella pneumophila resides within amoebae hosts in the natural environment. Here, we show that *L. pneumophila* injects an amylase to subvert the encystation of the amoebae natural host to maintain a permissive environment. Paradoxically, the amylase triggers an accidental pro-inflammatory response in the human host that modestly restricts bacterial replication.

Highlights

- *L. pneumophila* injects LamA, which degrades host cell glycogen

- LamA has evolved to interfere with amoebae host-specific processes

- In the amoebae natural host, LamA subverts encystation to promote a permissive host

- In humans, LamA triggers accidental inflammatory responses and nutritional immunity

CellPress

Article

CellPress

Paradoxical Pro-inflammatory Responses by Human Macrophages to an Amoebae Host-Adapted *Legionella* Effector

Christopher Price,[1] Snake Jones,[1] Mirna Mihelcic,[3] Marina Santic,[3] and Yousef Abu Kwaik[1,2,4,*]
[1]Department of Microbiology and Immunology, College of Medicine, University of Louisville, Louisville, KY, USA
[2]Center for Predictive Medicine, College of Medicine, University of Louisville, Louisville, KY, USA
[3]University of Rijeka, Rijeka, Croatia
[4]Lead Contact
*Correspondence: abukwaik@louisville.edu
https://doi.org/10.1016/j.chom.2020.03.003

SUMMARY

Legionella pneumophila has co-evolved with amoebae, their natural hosts. Upon transmission to humans, the bacteria proliferate within alveolar macrophages causing pneumonia. Here, we show *L. pneumophila* injects the effector LamA, an amylase, into the cytosol of human macrophage (hMDMs) and amoebae to rapidly degrade glycogen to generate cytosolic hyper-glucose. In response, hMDMs shift their metabolism to aerobic glycolysis, which directly triggers an M1-like pro-inflammatory differentiation and nutritional innate immunity through enhanced tryptophan degradation. This leads to a modest restriction of bacterial proliferation in hMDMs. In contrast, LamA-mediated glycogenolysis in amoebae deprives the natural host from the main building blocks for synthesis of the cellulose-rich cyst wall, leading to subversion of amoeba encystation. This is non-permissive for bacterial proliferation. Therefore, LamA of *L. pneumophila* is an amoebae host-adapted effector that subverts encystation of the amoebae natural host, and the paradoxical hMDMs' pro-inflammatory response is likely an evolutionary accident.

INTRODUCTION

The hallmarks of cells of the monocyte-macrophage lineage are their functional diversity and plasticity (Sica and Mantovani, 2012; Wynn et al., 2013). Depending on the signals *in vitro*, macrophages can undergo transient and reversible differentiation into two main subsets: "M1" pro-inflammatory/classically activated and "M2" anti-inflammatory/alternatively activated phenotype (Sica and Mantovani, 2012; Wang et al., 2014a; Wynn et al., 2013). M1 polarized mouse and human macrophages exhibit strong microbiocidal activity and produce pro-inflammatory cytokines such as TNF-α and interleukin (IL)-1β, IL-12, IL6, and IFN-γ, whereas M2 polarized macrophages are involved in parasite containment and tissue repair and produce anti-inflammatory cytokines such as IL-4, IL-10, and IL-13 (Price and Vance, 2014). Glucose is the primary source of energy in M1 polarized macrophages that reprogram their metabolism from oxidative phosphorylation into aerobic glycolysis (Warburg effect) with an increased production of lactate (Chang et al., 2013; Freemerman et al., 2014; Jha et al., 2015; Mills et al., 2016; Suzuki et al., 2016; Tannahill et al., 2013; Zhu et al., 2015).

A growing body of data *in vitro*, in animal models, and in diabetic patients show that excessive amounts of glucose triggers upregulation of aerobic glycolysis, which directly polarizes monocytes-macrophages toward a M1 pro-inflammatory phenotype (Bradshaw et al., 2009; Bustos and Sobrino, 1992; Haidet et al., 2012; Pan et al., 2012; Reinhold et al., 1996; Torres-Castro et al., 2016). Importantly, upon exposure of human monocytes/macrophages to high levels of glucose *in vitro*, they undergo M1 polarization along with an increased import of glucose, and monocytes/macrophages from patients with Type 1 diabetes exhibit a M1 pro-inflammatory profile (Erbel et al., 2016; Haidet et al., 2012; Kraakman et al., 2014; Pan et al., 2012; Reinhold et al., 1996; Torres-Castro et al., 2016).

In response to bacterial infections, macrophages undergo M1 pro-inflammatory polarization (Benoit et al., 2008; Hielpos et al., 2018; Mori et al., 2018; Yuan et al., 2019), which is an important arm of the innate host defense to restrict invading pathogens (Labonte et al., 2014; Benoit et al., 2008; Faris et al., 2019; Guo et al., 2019; Price and Vance, 2014; Sica and Mantovani, 2012; Yang et al., 2018). However, several facultative and obligate intracellular bacterial pathogens such as *Mycobacterium*, *Salmonella*, *Chlamydia*, *Coxiella*, *Brucella*, *Listeria*, and *Francisella* (Guo et al., 2019; Refai et al., 2018; Yuan et al., 2019) have evolved with mechanisms to interfere with M1 polarization of macrophages (Labonte et al., 2014; Benoit et al., 2008; Eisele et al., 2013; Muraille et al., 2014; Pathak et al., 2007; Price and Vance, 2014), but the mechanisms are not known. Paradoxically, macrophages respond to *Legionella pneumophila* by an inflammasome-independent rapid release of pro-inflammatory cytokines (Asrat et al., 2015; Asrat et al., 2014; Copenhaver et al., 2015; Fontana et al., 2011; Fontana et al., 2012; Ivanov and Roy, 2013; Price and Abu Kwaik, 2014; Rolando et al., 2013). However, the specific pathogenic signals of *L. pneumophila* or other intracellular pathogens that are sensed by macrophages to modulate M1/M2 differentiation are not known, and the mechanisms are not well understood.

L. pneumophila is an aquatic organism that has evolved to proliferate within amoebae as its primary natural host (Fields, 1996; Harb et al., 2000; Molmeret et al., 2005). The bacterium proliferates within the metabolically active trophozoite form of the amoeba (Bouyer et al., 2007; Kilvington and Price, 1990). Upon exposure to stress stimuli, such as nutrient depletion, metabolically active *Acanthamoeba* trophozoite differentiates into a double-walled cellulose-rich cyst (Byers et al., 1991; Lorenzo-Morales et al., 2008), which is a spore-like dormant form that completely restricts intracellular growth of *L. pneumophila* (Bouyer et al., 2007; Kilvington and Price, 1990). Although amoeba and other protists are considered the natural host for *L. pneumophila*, humans are considered to be an accidental host (Best and Abu Kwaik, 2018; Mori et al., 2018; Shuman et al., 1998; Swart et al., 2018). Upon inhalation of *L. pneumophila*-contaminated environmental aerosols by humans, the organism proliferates within alveolar macrophages causing pneumonia designated as Legionnaires' disease (Horwitz, 1983a, b; Horwitz and Silverstein, 1980). The intracellular lifestyle of *L. pneumophila* within amoebae and macrophages is very similar in that the organism is internalized into a phagosome that evades the endosomal-lysosomal pathway and intercepts early secretory vesicles to become an ER-derived vacuole, designated as the *Legionella*-containing vacuole (LCV) (Bärlocher et al., 2017; Haenssler et al., 2015; Isberg et al., 2009; Kagan and Roy, 2002; Kotewicz et al., 2017; Luo, 2011; Oliva et al., 2018; Richards et al., 2013).

The unique biogenesis of the LCV and modulation of plethora of cellular processes upon infection of amoebae and human macrophages is mediated by the Dot/Icm type IV secretion system that injects a cargo of >320 protein effectors into the host cells (Burstein et al., 2016; Schroeder, 2018; Zhu et al., 2011). *L. pneumophila* also utilizes a type II secretion system (T2SS) to secrete an array of 50 degradative and hydrolytic enzymes required for intracellular growth within amoeba, macrophages, and *in vivo* (Abu Khweek and Amer, 2018; Cianciotto and White, 2017; DebRoy et al., 2006; Rossier et al., 2004).

Most translocated effectors of *L. pneumophila* are not required for proliferation in human macrophages, and *L. pneumophila* have evolved to survive within their amoebae natural hosts, suggesting the effector repertoire is likely a toolbox to interact with various amoebal species (Best and Abu Kwaik, 2018; Park et al., 2020). Therefore, it is likely that the many amoebae-adapted effectors may cause accidental responses in human cells. Here, we show that the Dot/Icm injection machinery of intra-vacuolar *L. pneumophila* injects into the macrophage cytosol a *Legionella* amylase (Lam), LamA, that rapidly degrades cytosolic glycogen leading to a M1-like pro-inflammatory response, which partially restricts pathogen proliferation *ex vivo* and *in vivo*. In contrast to the paradoxical response of macrophages, LamA-mediated rapid glycogenolysis in the amoebae natural host subverts amoebae encystation. Therefore, LamA of *L. pneumophila* has evolved to be injected into the amoeba host to catalyze host glycogenolysis in order to subvert encystation of the amoebae natural host. However, the macrophage pro-inflammatory response is likely an evolutionary accident but with no major impact on disease manifestation.
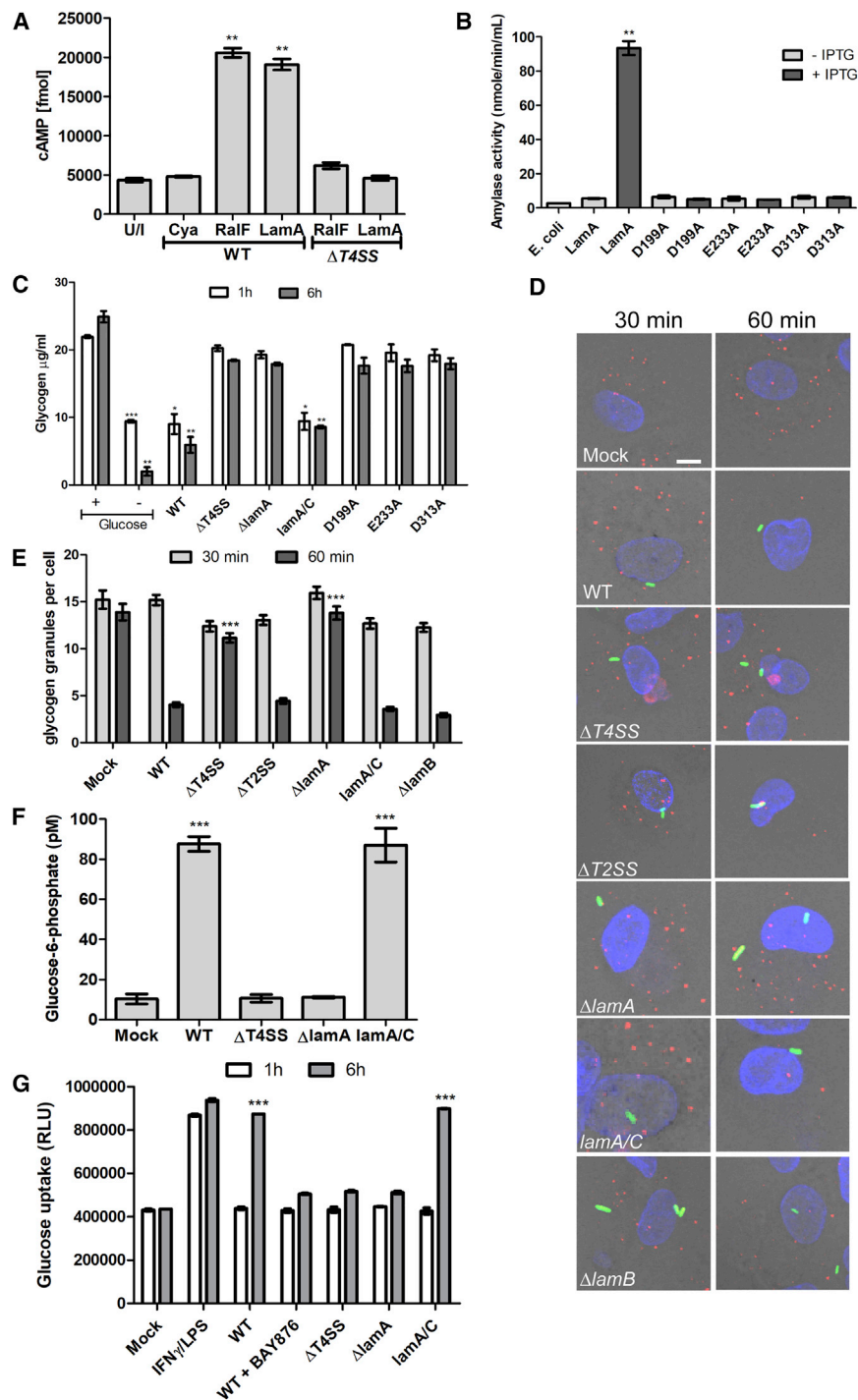
RESULTS

Dot/Icm Injection of a *Legionella* Amylase into the Macrophage Cytosol

Based on a potential putative translocation signal generated by a machine learning algorithm, many potential *L. pneumophila* candidates' effectors have been identified (Lifshitz et al., 2013). Two putative amylases (Lpg1671 and Lpg2528) were identified, but discounted, because there is no precedence for such an enzyme to be translocated into the host cell through type III–IX translocation systems of bacterial pathogens (Lifshitz et al., 2013). We have designated Lpg1671 and Lpg2528 as LamA and B (LamA and LamB), respectively. Because *L. pneumophila* does not synthesize glycogen or starch, we determined whether these amylases are injected into the host cell cytosol, using adenylate cyclase reporter fusions. We have previously shown that LamB is not translocated into the macrophage (Best et al., 2018). In contrast, we now show that LamA is translocated into the macrophage cytosol by wild-type bacteria but not by the type IV translocation-defective (ΔT4SS) mutant, similar to the RalF effector control (Figure 1A).

To confirm the enzymatic function of LamA, the native protein and three mutants with substitutions in the catalytic pocket (D199A, E233A, and D313A) were expressed in *E. coli* and the amylase activity was determined in total cell lysates. The data showed that LamA exhibited strong amylase activity, which was abolished by substitution of any of three residues in the catalytic pocket (Figures 1B and S1A). Taken together, the data show that LamA is a Dot/Icm-injected amylase, which is a unique example for such a hydrolytic enzyme of storage polymeric macromolecules to be injected into the host cell by type III–IX translocation machineries of bacterial pathogens.

Generation of Cytosolic Hyper-Glucose in hMDMs by LamA-Mediated Glycogenolysis

Glycogen is the sole glucose storage molecule in mammalian cells and is found in dense granules throughout the cytoplasm. We determined whether the pathogen-translocated LamA effector hydrolyzes macrophage glycogen. Human monocyte-derived macrophages (hMDMs) were infected with *L. pneumophila* and the quantity of glycogen was measured at 1 and 6 h post-infection. As expected, in hMDMs that were starved of glucose, glycogen was rapidly depleted within 1 h and was further reduced at 6 h following removal of glucose from the culture media, which is indicative of glycogenolysis (Figure 1C). Strikingly, in hMDMs infected with the wild-type strain of *L. pneumophila* for 1 h, glycogen was significantly depleted compared to uninfected cells (Student's t test, p = 0.0132) and was further reduced at 6 h post-infection (Student's t test, p = 0.0057) (Figure 1C). In contrast, glycogen levels in hMDMs infected with the translocation deficient ΔT4SS mutant or the Δ*lamA* mutant were unaffected and similar to uninfected cells at both 1 and 6 h post-infection (Figure 1C). Infection of hMDMs with the complemented Δ*lamA* mutant, *lamA/C*, resulted in rapid glycogen degradation, similar to that observed in cells infected with the wild-type strain (Figure 1C). However, infection of hMDMs with the Δ*lamA* mutant complemented with the catalytically dead variants of LamA did not result in glycogen

Figure 1. Generation of Cytosolic Hyper-Glucose in hMDMs by LamA-Mediated Glycogenolysis

(A) Adenylate cyclase (Cya) reporter fusion translocation assays of LamA expressed by wild-type *L. pneumophila* and the translocation-deficient ΔT4SS mutant. The Cya-RalF effector fusion was used as a positive control. hMDMs were in triplicate for 1 h, and cAMP production was assessed by ELISA. Data are shown as mean cAMP concentration ± SD, n = 3. ** Student's t test of wild-type RalF versus wild-type Cya, p < 0.0015; ** Student's t test of WT LamA versus WT Cya, p < 0.0024.

(B) Amylase activity was measured in lysates of *E. coli* expressing native or catalytic active site mutants GST-LamA fusions, with and without isopropyl β- d-1-thiogalactopyranoside (IPTG) induction, because expression was controlled by an IPTG-inducible promoter. Representative data of three independent experiments are shown as mean amylase activity ± SD, n = 3 independent cultures. ** Student's t test of IPTG-induced LamA versus un-induced LamA, p < 0.0021.

(C) Quantification of cytosolic glycogen concentrations in hMDMs starved of glucose or infected wild type, ΔT4SS, ΔlamA, or lamA/C and its catalytically inactive mutants at 1 and 6 h post-infection.

(D) Representative Z stack confocal microscopy images of hMDMs infected with various *L. pneumophila* strains (green) and glycogen granules were labeled by antibody (red). Scale bar represents 5 μm.

(E) Quantification of glycogen granules per infected cell at 30 and 60 min post-infection. Glycogen granules were counted in Z stack confocal images and data points show mean granules/infected cell ± SD, n = 100 infected cells, and are representative of three independent experiments. *** Student's t test of glycogen granules in either ΔT4SS- or ΔlamA-infected cells versus wild-type-infected cells, p < 0.0001.

(F) Quantification of cytosolic glucose-6-phosphate (G6P) levels in uninfected (U/I) and hMDMs infected with *L. pneumophila* strains. The data are representative of three independent experiments. *** Student's t test of G6P levels in either wild-type- or lamA/C-infected cells versus U/I infected cells, p < 0.0001.

(G) Determination of glucose uptake by hMDMs infected with the wild-type, ΔT4SS, ΔlamA, or lamA/C strains, or pretreated with LPS/IFN-γ at 1 and 6 h post-infection. BAY876 was used to block glucose transport *** Student's t test of glucose uptake levels in either wild-type- or lamA/C-infected cells versus mock, p < 0.0001.

degradation (Figure 1C). LamA-dependent glycogenolysis was further assessed by confocal microscopy. Following 30 min infection, uninfected hMDMs or hMDMs infected with wild-type strain, ΔT4SS, ΔlamA, or lamA/C mutants harbored between 10–15 dense glycogen granules (Figures 1D and 1E). Remarkably, at 1 and 2 h post-infection, hMDMs infected with the wild type or lamA/C harbored less than 5 glycogen granules, whereas the ΔT4SS- and ΔlamA-mutant-infected cells still harbored over

10 granules, similar to uninfected cells (Student's t test, p < 0.0001) (Figures 1D, 1E and S1B). A mutant defective in the T2SS (lspG) that is unable to secrete the glucoamylase, GamA (Herrmann et al., 2011; Rossier and Cianciotto, 2001), or defective for an alternate amylase, ΔlamB (Best et al., 2018), hydrolyzed host glycogen similar to the wild-type strain (Figures 1D, 1E, and S1B). Our data are clear that the Dot/Icm-translocated LamA catalyzes rapid glycogenolysis in macrophages.

To determine if the rapid LamA-mediated glycogenolysis results in elevation in cytosolic glucose, the level of glucose-6-phosphate (G6P) in infected hMDMs was determined. Following 1 h infection of hMDMs, the quantity of G6P in cells infected with wild-type bacteria increased by 5-fold compared to uninfected cells (Student's t test, p < 0.0001), whereas those infected with the ΔT4SS or ΔlamA mutant were similar to uninfected cells (Figure 1F). Importantly, infection of hMDMs with the complemented lamA/C strain resulted in high cytosolic G6P levels, similar to infection by the wild type (Student's t test, p < 0.0001) (Figure 1F). Taken together, LamA-mediated rapid glycogenolysis in macrophages results in cytosolic hyper-glucose.

Next, we determined if the rapid rise in cytosolic hyper-glucose within 1 h of infection is due to LamA-mediated glycogenolysis or if increased extracellular glucose uptake by hMDMs contributed to the cytosolic hyper-glucose. We measured glucose uptake by hMDMs infected with the wild-type, ΔT4SS, ΔlamA, or lamA/C strains at 1 h or 6 h post-infection or pre-stimulated with lipopolysaccharide (LPS)/IFN-γ for 24 h prior to the assay. We found at 1 h post-infection, glucose uptake by hMDMs infected with any of the L. pneumophila strains were similar to mock-infected cells (Figure 1G). However, at 6 h post-infection, hMDMs infected with the wild type or the lamA/C-complemented mutant strain exhibited a marked increase in glucose uptake compared to mock-infected cells (Student's t test, p = 0.0009, 0.0003 respectively). Importantly, elevated glucose uptake in wild-type-infected hMDMs was reversed when the cells were treated with a glucose transport inhibitor BAY876 (Figure 1G). In contrast, glucose uptake by hMDMs infected with the ΔT4SS or ΔlamA mutants for 6 h did not show increased glucose uptake (Figure 1G). As expected, hMDMs stimulated with LPS/IFN-γ showed elevated glucose uptake compared to mock-treated cells (Figure 1G). This shows that the initial rise in cytosolic hyper-glucose within 1 h of infection is due to LamA-mediated glycogenolysis and not uptake of extracellular glucose by hMDMs.

Partial Restriction of Pathogen Proliferation in Response to LamA-Dependent Cytosolic Hyper-Glucose

We determined the effect of LamA-mediated glycogenolysis on pathogen proliferation in hMDMs. By 24 h post-infection, the ΔlamA mutant exhibited 8-fold more intracellular bacteria than the wild-type strain, and this increased to over 12-fold at 48 h post-infection (Student's t test, p < 0.0001) (Figure 2A). Complementation of the ΔlamA mutant with the wild-type lamA gene but not the catalytically dead variants reversed the increased growth of the ΔlamA mutant, similar to that of the wild-type strain (Figure 2A). L. pneumophila expressed LamA and its catalytically dead variants equally (Figure S1C). Interestingly, the doubling time of the ΔlamA mutant (70 min) in hMDMs was significantly shorter than the wild-type strain (108 min) (Student's t test, p < 0.001), whereas growth of the ΔlamA mutant in rich bacteriological growth media was identical to the wild-type strain (Figure S1D). To confirm the intracellular replication phenotype of the ΔlamA mutant at the single-cell level, we assessed bacterial burden within LCVs at 6–8 h post-infection. At 6 h post-infection of hMDMs, LCVs harboring the wild-type strain had ~2 bacteria per LCV (Figures 2B and 2C). We observed a slight increase in bacterial number for LCVs harboring the ΔlamA mutant at 6 h
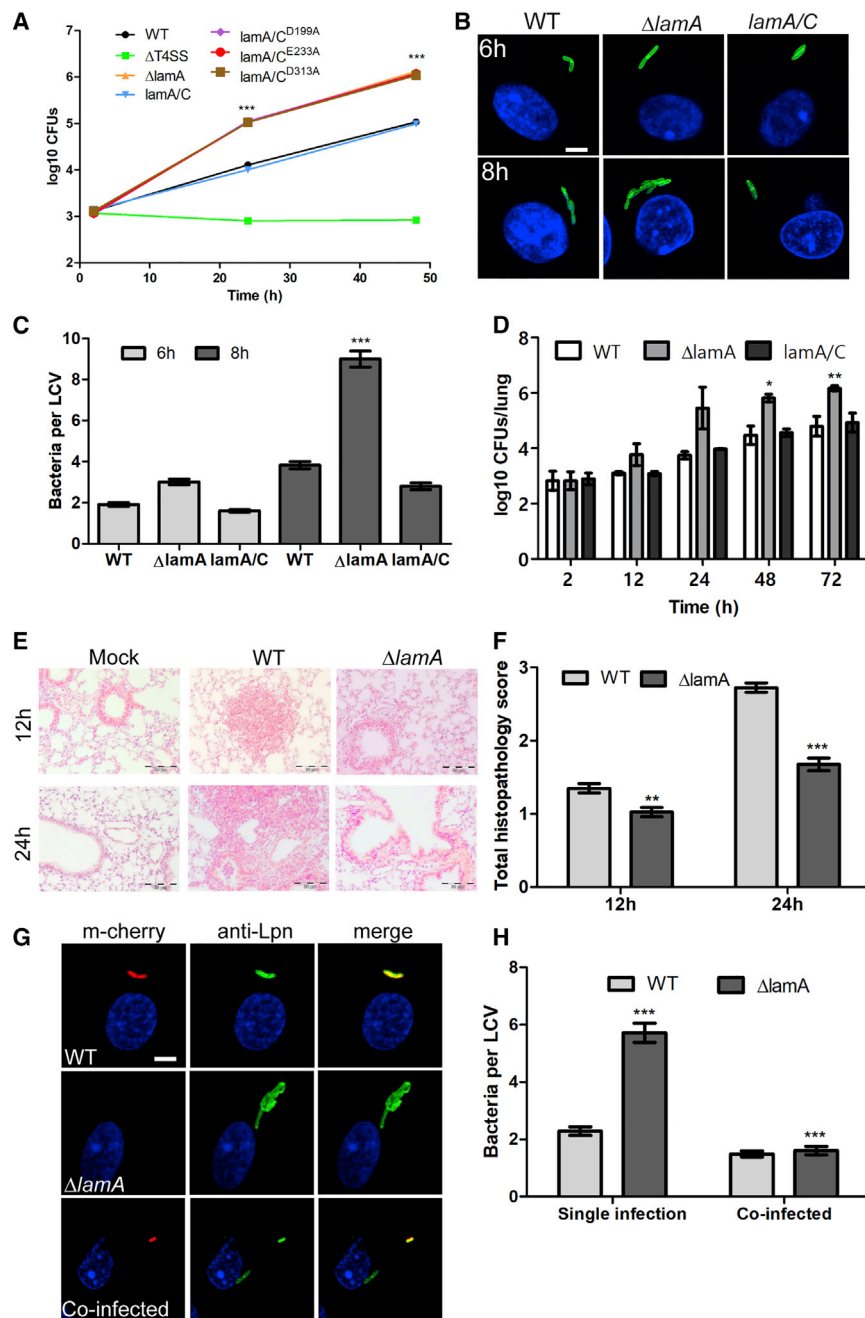
(~3 bacteria per LCV) but this was not significantly different from the wild-type strain (Student's t test, p > 0.12) (Figures 2B and 2C). However, at 8 h post-infection, LCVs harboring the ΔlamA mutant contained ~9 bacteria whereas those harboring the wild-type or the complemented lamA/C strain contained 4 bacteria (Student's t test, p < 0.0001) (Figures 2B and 2C). In contrast to what was observed in hMDMs, the ΔlamA mutant grew similarly to the wild-type strain in the natural host of L. pneumophila, Acanthamoeba polyphaga (Figure S2).

We determined the effect of LamA on intra-pulmonary growth of L. pneumophila in the A/J mouse model of disease after intratracheal inoculation of 10 animals per strain for each time point examined (Price and Abu Kwaik, 2010; Price et al., 2009). The data showed that the bacterial burden in the lungs and dissemination to the liver and spleen was significantly higher for the ΔlamA mutant compared to the wild-type and lamA/C strains (Figure 2D; Figures S3A and S3B). Surprisingly, there was no detectable effect on lethality, because 60% of mice infected by either the wild-type strain or the ΔlamA mutant succumbed to infection by 72 h (Figure S3C). Histopathology on pulmonary biopsies at 12 and 24 h post infection showed that the lungs of mice infected by the wild-type strain exhibited more severe inflammatory infiltrates within alveolar, bronchial, and peribronchial spaces with the infiltration of mononuclear cells (Figures 2E and 2F) than mice infected with the ΔlamA mutant strain (Student's t test, p < 0.05) (Figures 2E and 2F).

Glucose did not affect growth of L. pneumophila in bacteriological growth media (Figure S3D). To determine whether the cytosolic hyper-glucose microenvironment was responsible for partial restriction of intracellular growth of the wild-type strain, we attempted transfection with LamA, but its ectopic expression was toxic. Therefore, we performed co-infections of hMDMs with the wild-type bacteria and the ΔlamA mutant. When both strains co-inhabited the same cell, either within communal LCVs or within distinct LCVs, replication of the ΔlamA mutant was partially restricted, similar to the wild-type strain (Student's t test, p < 0.0001) (Figures 2G and 2H). Thus, the cytosolic hyper-glucose environment of macrophages partially restricts proliferation of L. pneumophila.

The hMDMs M1-like Pro-inflammatory Response to Cytosolic Hyper-Glucose

We tested the hypothesis that in response to the cytosolic hyper-glucose, hMDMs mount a pro-inflammatory response (Erbel et al., 2016; Haidet et al., 2012; Kraakman et al., 2014; Pan et al., 2012; Reinhold et al., 1996; Torres-Castro et al., 2016). At 6 h post-infection of hMDMs, the levels of pro- and anti-inflammatory cytokines released into the culture supernatant were measured. In response to infection with L. pneumophila, hMDMs released elevated levels of the pro-inflammatory cytokines IL-1α, IL-1β, IFN-γ, TNF-α, IL-12p40, and IL-12p70 compared to mock-infected cells (Figures 3A–3D and S4A). Importantly, in response to infection with the ΔlamA mutant, hMDMs released reduced levels of these six pro-inflammatory cytokines compared to those infected with the wild-type strain (Figures 3A–3D and S4A). Complementation of the ΔlamA mutant with the wild-type lamA gene but not the catalytically inactive mutant restored elevated release of cytokines by hMDMs (Figures 3A–3D and S4A). No differences were observed

Figure 2. LamA-Mediated Cytosolic Hyper-Glucose Restricts Pathogen Proliferation in hMDMs and *In Vivo*

Intra-vacuolar replication of wild type, Δ*T4SS*, Δ*lamA*, and *lamA/C* and the catalytically inactive mutants were assessed in hMDMs.

(A) To determine intra-vacuolar replication of *L. pneumophila*, infected hMDM monolayers were lysed at 2, 24, and 48 h post-infection and serial dilutions plated on agar plates to determine colony-forming unit (CFUs). Data shown are mean CFUs ± SD, n = 3, and are representative of three independent experiments. *** Student's t test of the number of *lamA* mutant bacteria versus wild type at 10 h, p < 0.0001.

(B and C) To further assess early time points for intra-vacuolar replication at the single-cell level, infected monolayers were fixed and immuno-stained for *L. pneumophila* (green), and bacterial numbers in replicative vacuoles were enumerated by confocal microscopy at 6 and 8 h post-infection. Representative confocal images are shown in (B), whereas quantification is shown in (C). Scale bar represents 5 μm. Data points show mean number of bacteria per LCV ± SD, n = 100 LCVs and are representative of three independent experiments. *** Student's t test of the number of *lamA* mutant bacteria per LCV at 8 h versus wild type, p < 0.0001.

(D) To assess intra-pulmonary proliferation of the *lamA* mutant, A/J mice were infected with 1×10^6 bacteria and the CFU burden in the lungs was assessed at various time points indicated. Data shown are mean CFUs ± SD per lung of three infected mice. Student's t test of the number of *lamA* mutant bacteria versus wild type at 48 h, *p < 0.0138 and at 72 h, **p < 0.0041.

(E) Representative images of pulmonary sections stained with hematoxylin and eosin. Scale bar represents 50 μm.

(F) Histopathology score of *lamA* infected lungs versus wild-type infected lungs 12 and 24 h post-infection; ** Student's t test, p < 0.0056 and at 24 h, ***p < 0.0001.

(G and H) Analysis of replicative LCVs within hMDMs co-infected with wild-type and *lamA* mutant bacteria using MOI 1:1 for the two strains and analyzed at 8 h post-infection using microscopic single-cell analyses. Representative confocal images of hMDMs infected with wild type or *lamA*, or co-infected with both strains. Infected monolayers were fixed and immunostained for *L. pneumophila* (green) and wild-type bacteria expressing m-Cherry (red). Scale bar represents

5 μm. Data points show mean number of bacteria per LCV ± SD, n = 100 LCVs, and are representative of three independent experiments. *** Student's t test of the number of *lamA* mutant/LCV versus wild-type bacteria at 8 h during individual infection with each strain compared to the number of *lamA* mutant bacteria in co-inhabited cells during co-infection, p < 0.0001.

for IL-6 secretion by hMDMs infected with any of the strains used (Figure S4A). In response to infection with *L. pneumophila*, hMDMs also released the M2 anti-inflammatory cytokines IL-4 and IL-10, but LamA did not play a role in the release of IL-4 and IL-10 (Figure S4B). Importantly, the bronchoalveolar lavage of mice infected with the wild-type strain contained elevated levels of TNF-α, IL-1α, IFN-γ and IL-6 compared to the *lamA* mutant infection (Student's t test, p < 0.0001) (Figures 3E and

S4C). However, production of IL-4 was increased in mice infected with the *lamA* mutant at 24 h post-infection compared to that observed for the wild-type strain (Student's t test, p < 0.0001), which suggested a more complex cytokine profile *in vivo* (Figure 3E) and may be due to differences between human and mouse macrophages.

We determined the potential of a paracrine effect of the secreted pro-inflammatory cytokines on bystander hMDMs to
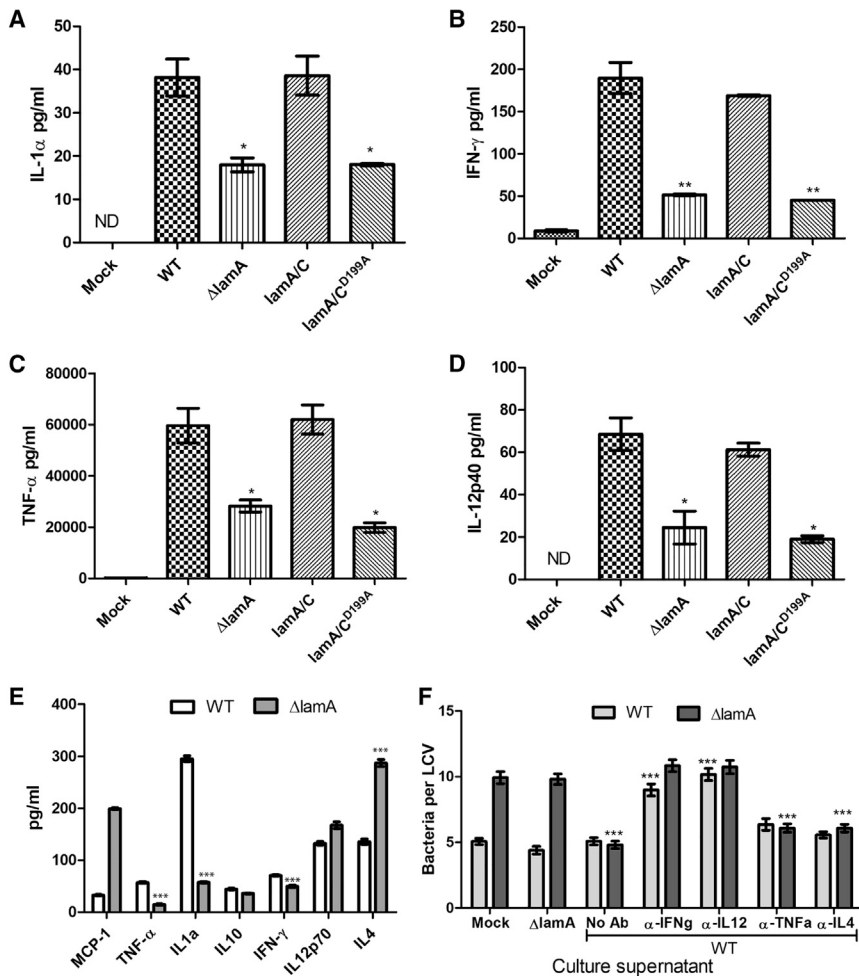
Figure 3. M1-like Pro-inflammatory Differentiation in Response to the Cytosolic Hyper-Glucose Generated by LamA-Mediated Glycogenolysis in hMDMs and *In Vivo*

(A–D) Selected panels of inflammatory cytokines (A) IL-1α, (B) IFN-γ, (C) TNF-α, and (D) IL12-p40, secreted by hMDMS infected for 6 h with wild type, *lamA*, *lamA/C*, or a catalytically inactive mutant were measured using a Milliplex assay. The rest of the cytokine panels are shown in Figure S4A. *** Student's t test of cytokine level in *lamA*-mutant-infected hMDMS compared to wild-type-infected cells, p < 0.0001.

(E) Cytokines levels in the bronchoalveolar lavage (BAL) at 24 h post-infection of mice. Data show pg/mL of cytokine present in BAL fluid. *** Student's t test of cytokine level in *lamA*-mutant-infected hMDMS compared to wild-type-infected mice, p < 0.0001.

(F) To determine a paracrine effect during infection of hMDMs, culture supernatants from mock-, wild-type–, or *lamA*-infected cells at 6 h were transferred to newly *lamA*-infected hMDMs for 8 h, and replicative vacuoles were assessed by confocal microscopy. For wild-type–infected supernatants, cytokines were neutralized by specific antibodies 1 h prior to infection. Data show mean number of bacteria per LCV ± SD, n = 100 LCVs, and are representative of three independent experiments. *** Student's t test of the number of *lamA* mutant bacteria per LCV with wild-type supernatant or TNFα/IL4-neutralized supernatants versus mock supernatant, or the number of wild-type bacteria per LCV with IFN-γ/IL12-neutralized wild-type supernatant versus wild-type supernatant, p < 0.0001.

restrict pathogen proliferation. Transfer of culture supernatants of 6 h infection by the wild-type strain to freshly infected hMDMs resulted in partial restriction of intracellular replication of the *ΔlamA* mutant, which was similar to the wild-type strain with only ∼5 bacteria per LCV at 8 h post-infection (Student's t test, p < 0.0001) (Figure 3F). In contrast, transfer of culture supernatants of hMDMs infected with the *ΔlamA* mutant for 6 h did not restrict intracellular replication of the *ΔlamA* mutant (Figure 3F). Neutralization of IFN-γ or IL-12 but not TNF-α or IL-4 in the transferred supernatant from wild-type strain infection reduced partial growth suppression of both the wild type and *ΔlamA* mutant strain in hMDMs with ∼8–10 bacteria per LCV (Student's t test, p < 0.0001) (Figure 3F).

Reprogramming hMDM Metabolism into Aerobic Glycolysis in Response to *L. pneumophila*

Pro-inflammatory M1 macrophages reprogram their metabolism into aerobic glycolysis, which leads to elevated secretion of lactate into the extracellular environment. The hMDMs infected with either the wild-type or *lamA/C* bacteria resulted in copious secretion of lactate into the culture supernatant by 6 h (157–175 nM) (Figure 4A), compared to infection by the *ΔlamA* or *ΔT4SS* mutants (23 nM) (Student's t test, p < 0.0001) (Figure 4A).

Because metabolic reprogramming into aerobic glycolysis is the driver for M1 pro-inflammatory polarization of macrophages, we determined the effect of inhibition of glycolysis on the LamA-dependent M1-like pro-inflammatory cytokine response and the partial restriction of pathogen proliferation. The data showed that prior inhibition of the glycolytic enzyme, enolase, by NaF abolished the LamA-dependent M1-like pro-inflammatory cytokine response of hMDMs (Student's t test, p < 0.0001) (Figures 4B and S5). Importantly, inhibition of hMDMs glycolysis by NaF or koningic acid, which inhibits enolase and glyceraldehyde 3-phosphate dehydrogenase respectively, enhanced replication of the wild-type strain, which phenocopied the *ΔlamA* mutant in mock-treated cells (Student's t test, p < 0.0001) (Figures 4C and 4D). The glycolysis inhibitors had no detectable effect on growth of *L. pneumophila* in broth culture *in vitro* (Figure S4D). Our data also showed that the wild-type strain triggered increased IFN-γ transcription compared to the *ΔlamA* mutant (21-fold versus 5-fold) relative to mock-infected cells (Figure 4E). Blocking glycolysis by NaF or koningic acid caused reduced IFN-γ transcription (−3.8-fold and −4.4-fold respectively) compared to mock-treated cells (Figure 4E). As expected, hMDMs pretreated with LPS/IFN-γ for 24 h prior to the assay exhibited increased IFN-γ transcription relative to mock-treated
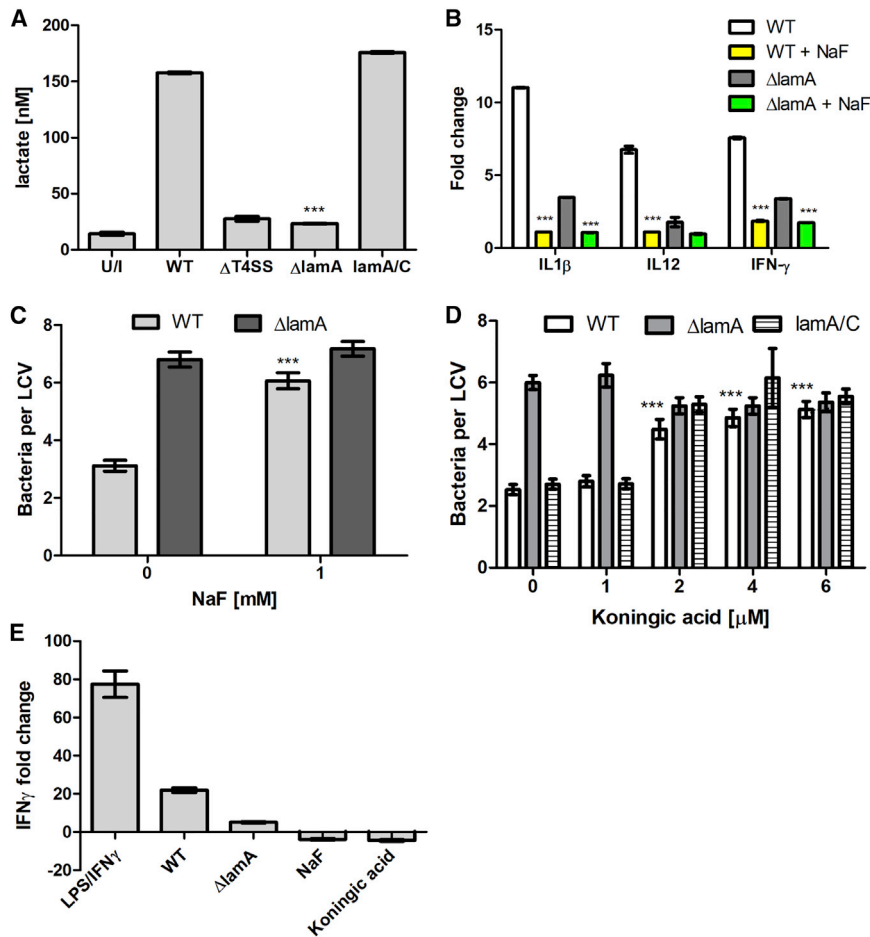
Figure 4. Upregulation of Aerobic Glycolysis in Response to the Cytosolic Hyper-Glucose Generated by LamA-Mediated Glycogenolysis Is Essential for M1-like Polarization of hMDMs

(A) Lactate levels in cell culture supernatants of hMDMS infected for 6 h with wild-type, ΔT4SS, ΔlamA, or lamA/C strains were assessed by ELISA. Data represent the mean lactate concentration ± SD, n = 3, and is representative of three independent experiments. *** Student's t test of lactate level in lamA-mutant-infected hMDMS compared to wild-type-infected cells, p < 0.0001.

(B) Selected panels of pro-inflammatory cytokines secreted by hMDMS in which glycolysis was inhibited by 1 mM NaF and infected for 6 h with wild type or ΔlamA were measured using a Multi-Analyte ELISArray kit and is representative of three independent experiments. The rest of the cytokine panels are shown in Figure S5. *** Student's t test of cytokine level in wild-type- or ΔlamA-mutant-infected hMDMS treated with NaF compared to untreated but infected cells, p < 0.0001.

(C and D) To assess the impact of hMDMs glycolysis on intra-vacuolar replication at the single-cell level, hMDMs were treated with NaF (C) or koningic acid (D) 1 h prior to and during infection. Replicative vacuoles were enumerated by confocal microscopy at 8 h post-infection. Data points show mean number of bacteria per LCV ± SD, n = 100 LCVs, and are representative of three independent experiments. *** Student's t test of the number of wild-type bacteria per LCV in treated cells versus untreated cells, p < 0.0001.

(E) Quantification of IFN-γ mRNA levels in hMDMs pre-treated with LPS/IFN-γ, infected with either the wild-type or ΔlamA mutant, or treated with glycolysis inhibitors NaF and koningic acid.

cells (Figure 4E). Our data indicate that in response to the cytosolic hyper-glucose generated by LamA-mediated glycogenolysis, hMDMs undergo M1-like pro-inflammatory polarization and partial restriction of pathogen proliferation.

Mechanism of LamA-Dependent Partial Suppression of *L. pneumophila* Replication

Pro-inflammatory macrophages restrict intracellular pathogens through multiple mechanisms including production of reactive oxygen species (ROS), increased lysosomal fusion, and restriction of nutrients such as tryptophan via increased indoleamine 2,3-dioxygenase 1 (IDO1) activity. The production of ROS by hMDMs infected with either wild-type or the ΔlamA mutant bacteria were similar to uninfected hMDMs (Figure S6A). Additionally, trafficking of both the wild-type and ΔlamA mutant bacteria in hMDMs showed that both equally evaded fusion to the lysosomes (Figure S6B). Next, we assessed expression of IDO1 in hMDMs infected with wild-type or ΔT4SS or ΔlamA mutant bacteria, or stimulated with LPS and IFN-γ at 2 and 4 h post-infection/treatment. At 4 h post-infection, there was a dramatic increase in IDO1 expression in hMDMs infected with wild-type bacteria, compared to the ΔlamA mutant or the translocation-deficient ΔT4SS mutant (Figure 5A). As expected, IDO1 expression was induced by LPS/IFN-γ stimulation control (Figure 5A).

Next, we measured the cytosolic concentration of tryptophan. Following 4 h of infection by the wild-type or lamA/C strain, the cytosolic concentration of tryptophan was reduced by 11-fold compared to hMDMs infected with ΔT4SS, ΔlamA or ΔlamA/ C$^{199D \rightarrow A}$, or mock-infected cells (Student's t test, p < 0.0001) (Figure 5B). Importantly, blocking IDO1 activity using 1-methyl-D-tryptophan (1-MDT) reversed depletion of tryptophan in hMDMs infected with the wild-type strain (Figure 5B).

We determined whether tryptophan supplementation would overcome the partial growth restriction of wild-type bacteria. Our data showed that at 8 h post-infection with wild-type bacteria in media with the standard concentration of tryptophan (90 μM) in RPMI 1640 cell culture media, each LCV harbored ∼4 bacteria (Figure 5C). However, supplementation of the culture media to a 180 or 360 μM tryptophan final concentration dramatically increased the number of wild-type bacteria per LCV (∼10 bacteria per LCV) (Student's t test, p < 0.0001), similar to LCVs harboring the ΔlamA mutant in regular media (Figure 5C). To confirm the role of IDO1-mediated nutritional restriction of *L. pneumophila* growth, hMDMs were treated with an IDO1 inhibitor prior to infection and intracellular replication was assessed at the single-cell level by confocal microscopy. At 6 h post-infection, LCVs harboring wild-type bacteria contained ∼2 bacteria. However, inhibition of IDO1 resulted in a
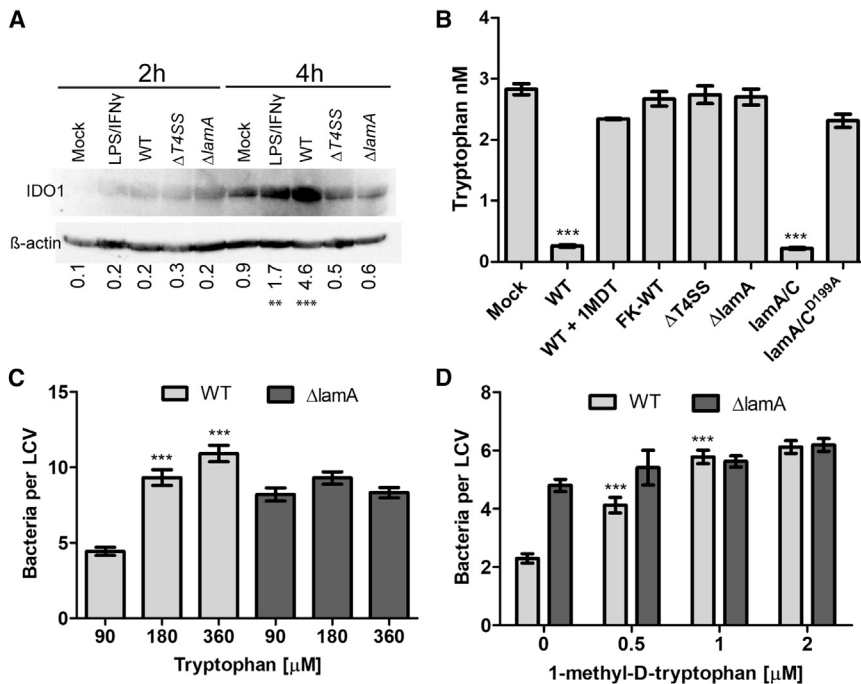
Figure 5. Induction of Innate Nutritional Immunity via Tryptophan Degradation in Response to the Cytosolic Hyper-Glucose Generated by LamA-Mediated Glycogenolysis

(A) Western blot of IDO1 expression in hMDMs infected with either wild type or ΔT4SS or ΔlamA mutants, or stimulated with LPS/IFNγ. β-actin served as a loading control. Numbers below loading control represent densitometry ratios of IDO1/actin. ** and *** Student's t test of the density ratio of LPS/IFN-γ and wild type at 4 h versus Mock at 4 h, p = 0.007, p < 0.0001 respectively, from three independent experiments.

(B) Quantification of cytosolic tryptophan concentrations in hMDMs infected with wild type, formalin-killed wild type, ΔT4SS, ΔlamA, lamA/C, and the catalytically inactive mutant 4 h post-infection. The IDO1 inhibitor 1-methy-D-tryptophan (1 mM) was added to wild-type-infected cells. Data points show mean tryptophan levels ± SD, n = 3, and are representative of three independent experiments. *** Student's t test of tryptophan concentration in wild-type- or lamA/C-infected cells versus mock, p < 0.0001.

(C) To determine if tryptophan supplementation enhanced intracellular replication of wild-type bacteria in hMDMs, cells were incubated with additional tryptophan supplement prior to infection and replicative LCVs were analyzed at 8 h post-infection by confocal microscopy at the single-cell level. Data points show mean number of bacteria per LCV ± SD, n = 100 LCVs, and are representative of three independent experiments. *** Student's t test of the number of wild-type bacteria per LCV at 180 or 360 μM tryptophan 8 h versus 90 μM tryptophan, p < 0.0001.

(D) To assess if IDO1 inhibition restored replication of wild-type bacteria, hMDMs were pretreated with increasing concentration of the inhibitor and infected with either the wild-type or ΔlamA mutant bacteria for 6 h. Data points show mean number of bacteria per LCV ± SD, n = 100 LCVs, and are representative of three independent experiments. * Student's t test of the number of wild-type bacteria per LCV at 0.5 or 1 μM inhibitor versus no inhibitor, p < 0.0001.

dose-dependent increase in wild bacteria replication (Student's t test, p < 0.0001), phenocopying the replication of the *lamA* mutant in untreated cells (Figure 5D). Thus, the modest LamA-dependent restriction in proliferation of wild-type *L. pneumophila* within the M1-like hMDMs is mainly due to innate nutritional immunity of IDO1-dependent tryptophan degradation and deprivation.

Subversion of Amoebae Host Encystation by Rapid LamA-Mediated Glycogenolysis

The LamA-dependent M1-like pro-inflammatory polarization and partial pathogen restriction seem to be counter-evolutionary for the adaptation of an intracellular pathogen to macrophages. These paradoxical findings lend credence to the hypothesis that it is more likely that LamA has evolved during co-evolution and adaptation of *L. pneumophila* with the amoebae natural host (Best and Abu Kwaik, 2018). Not surprisingly, phylogenetic analysis revealed that LamA, which is found in all sequenced *L. pneumophila* strains, is more closely related to amylases in *Acanthamoebae* than human amylases (Figure S7A), suggesting inter-kingdom horizontal gene transfer of *lamA* from an amoebae host into *L. pneumophila* (de Felipe et al., 2005; Franco et al., 2009).

We utilized *Acanthamoebae*, because they are the most widespread protist in nature and an established model host (Swart et al., 2018). Upon exposure to stress stimuli, vegetative metabolically active *Acanthamoeba* trophozoites progressively differentiate into an immature cyst with a minimal immature cellulose wall then to mature cysts characterized by their mature cellulose-rich double wall, which completely restrict intracellular growth of *L. pneumophila*. Synthesis of cellulose is essential for encystation and is accomplished by autophagy-mediated rapid glycogenolysis, which releases a high level of glucose to synthesize the cellulose-rich endocyst wall (Byers et al., 1991; Faber et al., 2017; Lorenzo-Morales et al., 2008; Moon et al., 2014; Schaap and Schilde, 2018). Because interference with glycogenolysis or cellulose biosynthesis block amoebae encystation (Byers et al., 1991; Collins et al., 1984; Faber et al., 2017; Lorenzo-Morales et al., 2008; Moon et al., 2014; Schaap and Schilde, 2018), we tested the hypothesis that LamA-mediated rapid glycogenolysis in the amoebae host interferes with encystation of amoebae, and this pathogenic property has evolved to maintain amoebae in the permissive trophozoite form. To determine if LamA triggered glycogenolysis in amoebae, G6P levels were measured. The data showed that at 1 h post-infection, there was little difference in G6P levels in infected amoebae compared to uninfected amoebae (Figure 6A). However, at 2 and 4 h post-infection, amoebae infected with the wild-type or the *lamA/C* strain exhibited significantly higher levels of G6P compared to those infected with the *ΔlamA* or ΔT4SS mutants (Student's t test, p < 0.0001), which were similar to uninfected amoebae (Figure 6A). As an indicator for elevated glycolysis, we determined lactate secretion by *A. polyphaga* infected with the wild type, the *ΔlamA* or ΔT4SS mutants, and the complemented *lamA/C* strain 4 h post-infection. The data show that *A. polyphaga*-infected with the wild type or *lamA/C*
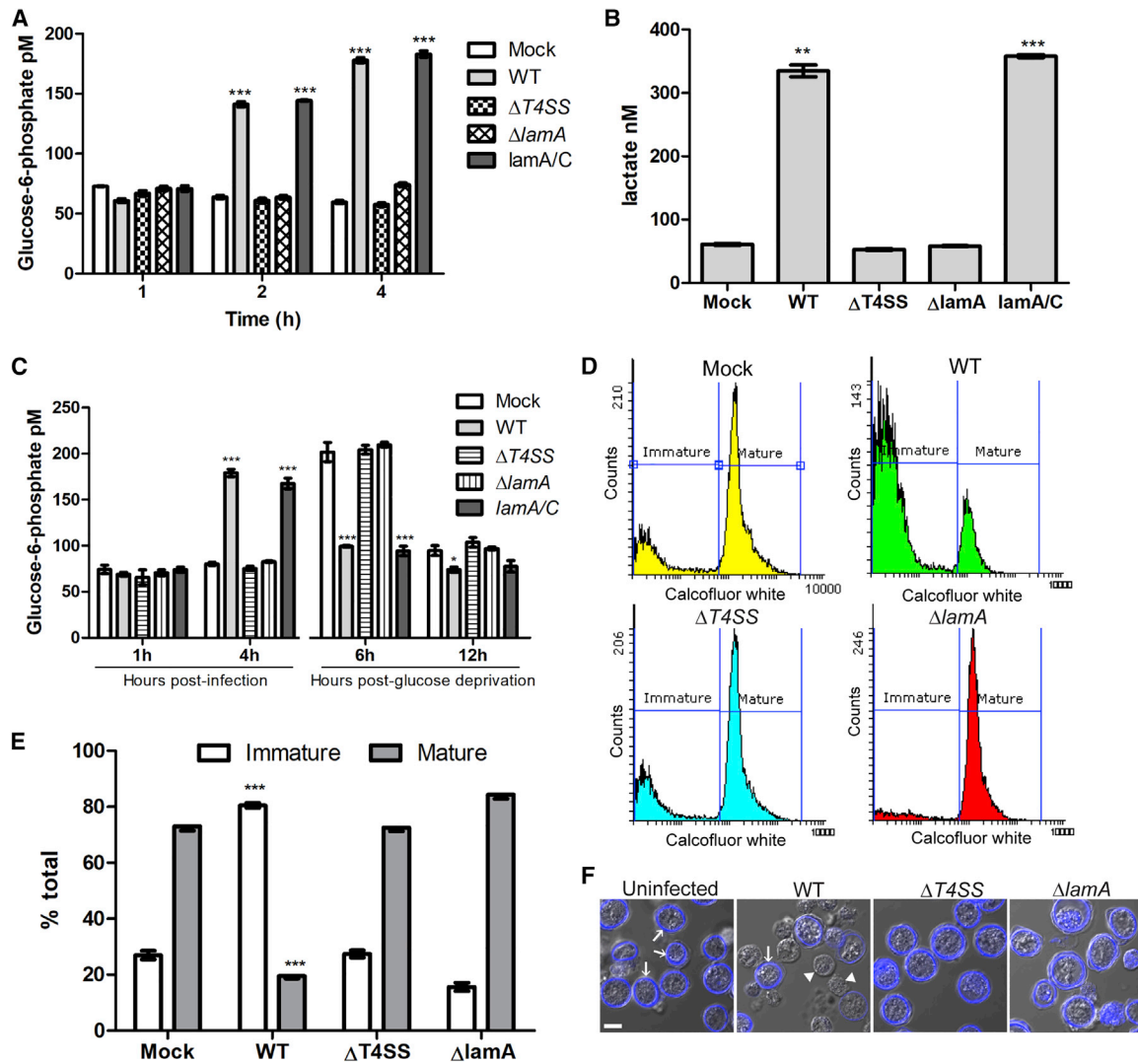
Figure 6. Interference with Encystation of *A. polyphaga* by LamA-Mediated Glycogenolysis

(A) Quantification of cytosolic G6P levels in *A. polyphaga* infected with *L. pneumophila*. The data are representative of three independent experiments. *** Student's t test of G6P levels in either wild-type- or *lamA/C*-infected cells versus U/l infected cells, p < 0.0001.

(B) Lactate levels in *A. polyphaga* culture supernatants infected for 4 h with wild-type, Δ*T4SS*, Δ*lamA*, or *lamA/C* strains were assessed by ELISA. Data represent the mean lactate concentration ± SD, n = 3, and is representative of three independent experiments. Student's t test of lactate level in wild-type- or *lamA/C*-infected *A. polyphaga* compared to mock-infected cells **p = 0.0012, ***p < 0.0001.

(C) Quantification of cytosolic G6P levels in *A. polyphaga* infected with *L. pneumophila* during encystation. Infected amoebae were infected for 4 h, and G6P levels were measured. Amoebae were then transferred to glucose-free encystation buffer, and G6P was measured 6 and 12 h post-encystation. *** Student's t test of G6P levels in either wild-type- or *lamA/C*-infected cells versus mock-infected cells, p < 0.0001.

(D and E) To assess development of amoebae cysts following infection by *L. pneumophila*, *A. polyphaga* were labeled with Calcofluor White, which intensely stains the dense cellulose wall of endocysts, and subjected to flow cytometry. Flow cytometry histograms of U/l *A. polyphaga* or infected with wild-type bacteria or the Δ*T4SS* and Δ*lamA* mutants 2 days post-incubation in encystation media are shown (D), and quantification is shown in (E). The data are representative of three independent experiments. *** Student's t test of immature or mature cysts in wild-type-infected cells versus mock, p < 0.0001.

(F) Representative confocal images of *A. polyphaga* cysts following infection with the wild type or the Δ*T4SS* and Δ*lamA* mutants three days post-incubation in encystation media. Mature cysts (arrows) are characterized by intense endocyst wall staining (blue), whereas immature precysts (arrowheads) or non-encysted amoebae stain weakly or do not stain. Scale bar represents 5 μm.

secrete significantly more lactate than those infected with the Δ*lamA* or Δ*T4SS* mutants or mock-infected cells (Student's t test, p = 0.0012, p < 0.0001) (Figure 6B). This indicates that similar to hMDMs, increased glycolysis in *A. polyphaga* is triggered by LamA-catalyzed rapid glycogenolysis.

Next, we determined if depletion of glycogen in trophozoites infected with the wild-type strain prior to encystation stimuli impacts availability of glucose needed for the biosynthesis of the cellulose rich endocyst wall. To achieve this, *A. polyphaga* trophozoites were infected with the wild-type, Δ*T4SS*, Δ*lamA*, and *lamA/C*

strains for 4 h in culture media containing glucose. At 1 h post-infection, G6P levels in all conditions were similar, but at 4 h, G6P levels in wild-type and *lamA/C*-infected *A. polyphaga* trophozoites were significantly elevated (Student's t test, p < 0.0001) compared to mock-infected cells (Figure 6C). At 4 h post-infection, the infected trophozoites were transferred to glucose-free encystation buffer, and G6P levels were measured at 6 h, 12 h, and 24 h post-encystation. At 6 h post-glucose deprivation, G6P levels in mock-infected or ΔT4SS- or Δ*lamA*-mutant-infected *A. polyphaga* were elevated compared to pre-encystation levels. In contrast, G6P levels in *A. polyphaga* infected with the wild-type or *lamA/C* strains were significantly reduced (Student's t test, p < 0.0001) (Figure 6C). At 12 h post-glucose deprivation, the G6P levels in mock-infected or ΔT4SS- or Δ*lamA*-mutant-infected *A. polyphaga* had reduced to a similar level seen for wild-type or *lamA/C*-infected *A. polyphaga* (Figure 6C). These data indicate that LamA-dependent depletion of glycogen in wild-type *L. pneumophila*-infected *A. polyphaga* reduces the availability of glucose required for encystation of amoebae.

The impact of rapid LamA-mediated depletion of glycogen prior to amoebae encystation was determined by flow cytometry analysis and by confocal microscopy. *A. polyphaga* were labeled with Calcofluor White, which intensely stains the dense cellulose wall of mature endocysts. Following 2 h infection of *A. polyphaga* by *L. pneumophila* and 2 days incubation in glucose-free encystation buffer, >80% of *A. polyphaga* infected with either Δ*lamA* or ΔT4SS mutant formed mature cysts characterized by dense cellulose endocyst walls, similar to uninfected amoebae (Figures 6D–6F). In contrast, only ~20% of *A. polyphaga* infected with wild-type *L. pneumophila* formed mature cysts (Figures 6D–6F) (Student's t test, p < 0.0001) with most amoebae in a cellulose-depleted immature precyst form, indicating interference with amoebal encystation as a result of rapid LamA-mediated glycogenolysis. Similar results were observed 3 days post-encystation (Figure S7B). It was observed that trypan blue dye exclusion and counting show no reduction in amoebal viability and no increase in *L. pneumophila* populations (data not shown). Taken together, the data indicate that LamA has evolved to modulate an amoeba-specific process that is absent in the more evolved accidental human host, and LamA has likely played a key role in co-evolution and adaptation of *L. pneumophila* with the amoebae natural hosts. However, the paradoxical macrophage response to the cytosolic hyper-glucose generated by LamA-mediated glycogenolysis is likely an unintended evolutionary accident with no major outcome on disease manifestation. It is not known whether the cytosolic hyper-glucose in the amoebae host has effects on amoebae cellular processes beyond subverting encystation.

DISCUSSION

L. pneumophila reside in a wide range of amoebae species in the environment and has acquired a large repertoire of effector proteins that it utilizes to survive and proliferate within these host cells (Best and Abu Kwaik, 2018). It may not be surprising that most effector mutants of *L. pneumophila* are not defective in macrophages, given that most effectors have likely evolved to adapt to various protist hosts in the environment (Best and Abu Kwaik, 2018; Park et al., 2020). Many effectors modulate conserved pro-

cesses in both macrophages and amoebae, but no effector has been shown to modulate cellular processes specific to amoebae that are absent in the more evolved human host. Amoebae respond to nutrient deprivation by formation of dormant metabolically inactive cysts (Schaap and Schilde, 2018), which are non-permissive for *L. pneumophila* (Bouyer et al., 2007; Kilvington and Price, 1990). We show here that the injected LamA catalyzes rapid glycogenolysis in amoebae and glycogen depletion blocks the ability of amoebae to form mature cysts, suggesting evolutionary selection pressure of LamA to maintain amoebae hosts in the permissive trophozoite form. However, the environmental selection for an injected amylase that targets host glycogen has led to an unintended and paradoxical consequence when *L. pneumophila* encounters human macrophages.

When *L. pneumophila* invades human macrophages, it translocates LamA causing glycogenolysis with abnormal rise in cytosolic glucose. However, unlike amoebae, the response to cytosolic hyper-glucose in infected macrophages triggers aerobic glycolysis, which triggers a rapid M1-like pro-inflammatory differentiation. This may mimic the M1 pro-inflammatory polarization of macrophages upon exposure to high levels of glucose (Erbel et al., 2016; Haidet et al., 2012; Kraakman et al., 2014; Pan et al., 2012; Reinhold et al., 1996; Torres-Castro et al., 2016). Although import of extracellular glucose represents a bottleneck, LamA-mediated hyper-glucose bypasses the glucose import bottleneck. In addition to the critical role of LamA, *L. pneumophila* targets mitochondrial dynamics to promote a Warburg-like phenotype in macrophages (Escoll et al., 2017; Price et al., 2018). Interestingly, macrophages infected with *L. pneumophila* produce a number of cytokines even though this bacteria injects several effectors that block host protein synthesis (Asrat et al., 2014; De Leon et al., 2017; Shen et al., 2009). To overcome this blockade, macrophages infected with wild-type *L. pneumophila* produce IL-1α, which signals uninfected bystander cells to produce pro-inflammatory cytokines such as IL-6, TNF-α, and IL12, which are made poorly by the infected cells (Copenhaver et al., 2015). Our data show that several pro-inflammatory cytokines are made by hMDMs in response to infection by the wild-type strain, and this is dependent on the catalytic activity of LamA. It is important to note that our infection model routinely results in at least 95% of the hMDMs infected with *L. pneumophila*, but we cannot exclude the possibility that the 1%–5% of uninfected bystander cells may contribute to the production of pro-inflammatory cytokines.

To restrict replication of invading bacterial pathogens, pro-inflammatory macrophages employ a variety of mechanisms including increased efficacy of lysosomal degradation, increased ROS killing ability, and elevated IDO1 activity. Despite a robust pro-inflammatory macrophage response, wild-type *L. pneumophila* utilizes a powerful lysosomal bypass pathway to avoid degradation within lysosomes of M1-like pro-inflammatory macrophages (Ensminger, 2016). Despite reliance of *L. pneumophila* on host amino acids (Price et al., 2011), *L. pneumophila* is auxotrophic for many amino acids, highlighting the necessity of this pathogen to acquire amino acids from its host (Fonseca and Swanson, 2014; Price et al., 2011). Although *L. pneumophila* is not auxotrophic for tryptophan, acquisition of tryptophan from the host, in addition to *de novo* synthesis by the bacteria, is required for optimal intracellular

growth (Jones et al., 2015). The LamA-mediated pro-inflammatory response of infected hMDMs (IFN-γ in particular) triggers IFN-γ-mediated IDO1 expression leading to depletion of host tryptophan (Wang et al., 2014b), which is responsible for the partial growth restriction through nutritional innate immunity. Because >95% of the macrophages are infected with *L. pneumophila*, it is likely that translation of IDO1 in infected cells overcomes the protein synthesis block, similar to that observed for pro-inflammatory cytokines (Asrat et al., 2014). IDO1-mediated tryptophan depletion also limits *Toxoplasma*, *Chlamydia*, and *Leishmania* replication (Dai et al., 1994; Murray et al., 1989; Thomas et al., 1993). Therefore, the IFN-γ-mediated elevated IDO1 expression and tryptophan depletion are the mechanisms of nutritional innate immunity that partially restrict robust intracellular replication of *L. pneumophila*.

Besides LamA, *L. pneumophila* harbors two other characterized amylases. The glucoamylase, GamA, is secreted by the type II secretion system but does not impact intracellular growth (Herrmann et al., 2011). We show that GamA is not involved in glycogenolysis. Additionally, *L. pneumophila* expresses LamB, which is not injected into the host cytosol but is required for bacterial replication in amoebae, human macrophages, and the murine model of disease via an unknown mechanism (Best et al., 2018). Therefore, LamA is the major factor of *L. pneumophila* responsible for glycogenolysis during infection of host cells. However, it is possible that other *L. pneumophila* effectors and/or host cell signaling pathways may contribute to *L. pneumophila*-induced glycogenolysis. Amylase and glycosidase activity has also been shown to contribute to the pathogenesis of other bacterial pathogens, but they act on complex extracellular glycans (Arabyan et al., 2016; Marion et al., 2009; Robb et al., 2017). In contrast to LamA-mediated glycogenolysis, the obligate intracellular pathogen, *Chlamydia trachomatis*, shifts host glycogen stores to its replicative vacuole through bulk uptake and *de novo* synthesis from host-derived UDP-glucose (Gehre et al., 2016). *C. trachomatis* translocates bacterial glycogen biosynthesis enzymes into the lumen of its replicative vacuole via its type III secretion system, generating an energy store, which is derived from the host, for the metabolic benefit of the bacterial pathogen (Gehre et al., 2016).

Our data provide strong evidence for manipulation of amoebae-specific cellular processes and intimate co-evolution of *L. pneumophila* with its amoebae natural hosts. Because the dormant cyst form of amoebae is non-permissive for proliferation of *L. pneumophila*, the pathogen has evolved to inject LamA into the amoebae host, triggering rapid glycogenolysis to subvert host encystation and promote pathogen proliferation within the permissive trophozoite form. The macrophage M1-like pro-inflammatory differentiation and nutritional innate immunity in response to *Legionella*-mediated glycogenolysis is paradoxical and counter evolutionary, but not detrimental, and is likely an evolutionarily unintended or accidental event.

STAR★METHODS

Detailed methods are provided in the online version of this paper and include the following:

- KEY RESOURCES TABLE
- LEAD CONTACT AND MATERIALS AVAILABILITY
- EXPERIMENTAL MODEL AND SUBJECT DETAILS
  - Isolation of Human Monocyte-Derived Macrophages
  - A/J Mouse Model
  - Microbial Strains
- METHOD DETAILS
  - Generation of a *lamA* Knockout Mutant
  - Translocation Assay
  - Amylase Activity Assay
  - Analysis of Intracellular Glycogen
  - Determination of Cytosolic Glucose-6-phosphate
  - Glucose Uptake Assay
  - *In Vitro* Broth Culture Growth Curves
  - Intracellular Replication
  - Co-infection of hMDMs with Wild Type and *lamA* Bacteria
  - Determination of Secreted Lactate by Infected hMDMs
  - Analysis of Indoleamine 2,3-dioxygenase
  - Analysis of Reactive Oxygen Species Production and Intracellular Trafficking of *L. pneumophila*
  - Cytokine Analysis
  - Mouse Model of Infection
  - Encystation of *Acanthamoeba polyphaga* Infected with *L. pneumophila*
- QUANTIFICATION AND STATISTICAL ANALYSIS
- DATA AND CODE AVAILABILITY

AUTHOR CONTRIBUTIONS

C.P., S.J., and M.S. performed the experiments; C.P., S.J., M.S., and Y.A.K. analyzed the data; and Y.A.K. supervised the project. All authors wrote the manuscript.

DECLARATION OF INTERESTS

The authors declare no competing interests.

REFERENCES

Abu Khweek, A., and Amer, A.O. (2018). Factors Mediating Environmental Biofilm Formation by *Legionella pneumophila*. Front. Cell. Infect. Microbiol. *8*, 38.

Al-Khodor, S., Price, C.T., Habyarimana, F., Kalia, A., and Abu Kwaik, Y. (2008). A Dot/Icm-translocated ankyrin protein of Legionella pneumophila is required for intracellular proliferation within human macrophages and protozoa. Mol. Microbiol. *70*, 908–923.

Arabyan, N., Park, D., Foutouhi, S., Weis, A.M., Huang, B.C., Williams, C.C., Desai, P., Shah, J., Jeannotte, R., Kong, N., et al. (2016). Salmonella Degrades the Host Glycocalyx Leading to Altered Infection and Glycan Remodeling. Sci. Rep. *6*, 29525.

Asrat, S., Dugan, A.S., and Isberg, R.R. (2014). The frustrated host response to Legionella pneumophila is bypassed by MyD88-dependent translation of pro-inflammatory cytokines. PLoS Pathog. *10*, e1004229.

Asrat, S., Davis, K.M., and Isberg, R.R. (2015). Modulation of the host innate immune and inflammatory response by translocated bacterial proteins. Cell. Microbiol. *17*, 785–795.

Bärlocher, K., Welin, A., and Hilbi, H. (2017). Formation of the *Legionella* Replicative Compartment at the Crossroads of Retrograde Trafficking. Front. Cell. Infect. Microbiol. *7*, 482.

Benoit, M., Desnues, B., and Mege, J.-L. (2008). Macrophage polarization in bacterial infections. J. Immunol. *181*, 3733–3739.

Best, A., and Abu Kwaik, Y. (2018). Evolution of the arsenal of Legionella pneumophila effectors to modulate protist hosts. MBio *9*, e01313–e01318.

Best, A., Price, C., Ozanic, M., Santic, M., Jones, S., and Abu Kwaik, Y. (2018). A Legionella pneumophila amylase is essential for intracellular replication in human macrophages and amoebae. Sci. Rep. *8*, 6340.

Bouyer, S., Imbert, C., Rodier, M.H., and Héchard, Y. (2007). Long-term survival of Legionella pneumophila associated with Acanthamoeba castellanii vesicles. Environ. Microbiol. *9*, 1341–1344.

Bradshaw, E.M., Raddassi, K., Elyaman, W., Orban, T., Gottlieb, P.A., Kent, S.C., and Hafler, D.A. (2009). Monocytes from patients with type 1 diabetes spontaneously secrete proinflammatory cytokines inducing Th17 cells. J. Immunol. *183*, 4432–4439.

Burstein, D., Amaro, F., Zusman, T., Lifshitz, Z., Cohen, O., Gilbert, J.A., Pupko, T., Shuman, H.A., and Segal, G. (2016). Genomic analysis of 38 Legionella species identifies large and diverse effector repertoires. Nat. Genet. *48*, 167–175.

Bustos, R., and Sobrino, F. (1992). Stimulation of glycolysis as an activation signal in rat peritoneal macrophages. Effect of glucocorticoids on this process. Biochem. J. *282*, 299–303.

Byers, T.J., Kim, B.G., King, L.E., and Hugo, E.R. (1991). Molecular aspects of the cell cycle and encystment of *Acanthamoeba*. Rev. Infect. Dis. *13* (*Suppl 5*), S373–S384.

Chang, C.-H., Curtis, J.D., Maggi, L.B., Jr., Faubert, B., Villarino, A.V., O'Sullivan, D., Huang, S.C., van der Windt, G.J., Blagih, J., Qiu, J., et al. (2013). Posttranscriptional control of T cell effector function by aerobic glycolysis. Cell *153*, 1239–1251.

Chen, D.Q., Huang, S.S., and Lu, Y.J. (2006). Efficient transformation of Legionella pneumophila by high-voltage electroporation. Microbiol. Res. *161*, 246–251.

Cianciotto, N.P., and White, R.C. (2017). The Expanding Role of Type II Secretion in Bacterial Pathogenesis and Beyond. Infect Immun *85*, https://doi.org/10.1128/IAI.00014-17.

Collins, M.T., McDonald, J., Høiby, N., and Aalund, O. (1984). Agglutinating antibody titers to members of the family Legionellaceae in cystic fibrosis patients as a result of cross-reacting antibodies to Pseudomonas aeruginosa. J. Clin. Microbiol. *19*, 757–762.

Copenhaver, A.M., Casson, C.N., Nguyen, H.T., Duda, M.M., and Shin, S. (2015). IL-1R signaling enables bystander cells to overcome bacterial blockade of host protein synthesis. Proc. Natl. Acad. Sci. USA *112*, 7557–7562.

Dai, W., Pan, H., Kwok, O., and Dubey, J.P. (1994). Human indoleamine 2,3-dioxygenase inhibits Toxoplasma gondii growth in fibroblast cells. J. Interferon Res. *14*, 313–317.

de Felipe, K.S., Pampou, S., Jovanovic, O.S., Pericone, C.D., Ye, S.F., Kalachikov, S., and Shuman, H.A. (2005). Evidence for acquisition of Legionella type IV secretion substrates via interdomain horizontal gene transfer. J. Bacteriol. *187*, 7716–7726.

De Leon, J.A., Qiu, J., Nicolai, C.J., Counihan, J.L., Barry, K.C., Xu, L., Lawrence, R.E., Castellano, B.M., Zoncu, R., Nomura, D.K., et al. (2017). Positive and Negative Regulation of the Master Metabolic Regulator mTORC1 by Two Families of Legionella pneumophila Effectors. Cell Rep. *21*, 2031–2038.

De Simone, M., Spagnuolo, L., Lorè, N.I., Rossi, G., Cigana, C., De Fino, I., Iraqi, F.A., and Bragonzi, A. (2014). Host genetic background influences the response to the opportunistic Pseudomonas aeruginosa infection altering cell-mediated immunity and bacterial replication. PLoS ONE *9*, e106873.

DebRoy, S., Dao, J., Söderberg, M., Rossier, O., and Cianciotto, N.P. (2006). Legionella pneumophila type II secretome reveals unique exoproteins and a chitinase that promotes bacterial persistence in the lung. Proc. Natl. Acad. Sci. USA *103*, 19146–19151.

Eisele, N.A., Ruby, T., Jacobson, A., Manzanillo, P.S., Cox, J.S., Lam, L., Mukundan, L., Chawla, A., and Monack, D.M. (2013). Salmonella require the fatty acid regulator PPARδ for the establishment of a metabolic environment essential for long-term persistence. Cell Host Microbe *14*, 171–182.

Ensminger, A.W. (2016). Legionella pneumophila, armed to the hilt: justifying the largest arsenal of effectors in the bacterial world. Curr. Opin. Microbiol. *29*, 74–80.

Erbel, C., Rupp, G., Domschke, G., Linden, F., Akhavanpoor, M., Doesch, A.O., Katus, H.A., and Gleissner, C.A. (2016). Differential regulation of aldose reductase expression during macrophage polarization depends on hyperglycemia. Innate Immun. *22*, 230–237.

Escoll, P., Song, O.-R., Viana, F., Steiner, B., Lagache, T., Olivo-Marin, J.-C., Impens, F., Brodin, P., Hilbi, H., and Buchrieser, C. (2017). Legionella pneumophila Modulates Mitochondrial Dynamics to Trigger Metabolic Repurposing of Infected Macrophages. Cell Host Microbe *22*, 302–316.e7.

Faber, K., Zorzi, G.K., Brazil, N.T., Rott, M.B., and Teixeira, H.F. (2017). siRNA-loaded liposomes: Inhibition of encystment of Acanthamoeba and toxicity on the eye surface. Chem. Biol. Drug Des. *90*, 406–416.

Faris, R., Andersen, S.E., McCullough, A., Gourronc, F., Klingelhutz, A.J., and Weber, M.M. (2019). *Chlamydia trachomatis* Serovars Drive Differential Production of Proinflammatory Cytokines and Chemokines Depending on the Type of Cell Infected. Front. Cell. Infect. Microbiol. *9*, 399.

Fields, B.S. (1996). The molecular ecology of legionellae. Trends Microbiol. *4*, 286–290.

Fonseca, M.V., and Swanson, M.S. (2014). Nutrient salvaging and metabolism by the intracellular pathogen Legionella pneumophila. Front. Cell. Infect. Microbiol. *4*, 12.

Fontana, M.F., Banga, S., Barry, K.C., Shen, X., Tan, Y., Luo, Z.Q., and Vance, R.E. (2011). Secreted bacterial effectors that inhibit host protein synthesis are critical for induction of the innate immune response to virulent Legionella pneumophila. PLoS Pathog. *7*, e1001289.

Fontana, M.F., Shin, S., and Vance, R.E. (2012). Activation of host mitogen-activated protein kinases by secreted Legionella pneumophila effectors that inhibit host protein translation. Infect. Immun. *80*, 3570–3575.

Franco, I.S., Shuman, H.A., and Charpentier, X. (2009). The perplexing functions and surprising origins of Legionella pneumophila type IV secretion effectors. Cell. Microbiol. *11*, 1435–1443.

Freemerman, A.J., Johnson, A.R., Sacks, G.N., Milner, J.J., Kirk, E.L., Troester, M.A., Macintyre, A.N., Goraksha-Hicks, P., Rathmell, J.C., and Makowski, L. (2014). Metabolic reprogramming of macrophages: glucose transporter 1 (GLUT1)-mediated glucose metabolism drives a proinflammatory phenotype. J. Biol. Chem. *289*, 7884–7896.

Gebhardt, M.J., Jacobson, R.K., and Shuman, H.A. (2017). Seeing red; the development of pON.mCherry, a broad-host range constitutive expression plasmid for Gram-negative bacteria. PLoS ONE *12*, e0173116.

Gehre, L., Gorgette, O., Perrinet, S., Prevost, M.C., Ducatez, M., Giebel, A.M., Nelson, D.E., Ball, S.G., and Subtil, A. (2016). Sequestration of host metabolism by an intracellular pathogen. eLife *5*, e12552.

Guo, Q., Bi, J., Li, M., Ge, W., Xu, Y., Fan, W., Wang, H., and Zhang, X. (2019). ESX Secretion-Associated Protein C From *Mycobacterium tuberculosis* Induces Macrophage Activation Through the Toll-Like Receptor-4/Mitogen-Activated Protein Kinase Signaling Pathway. Front. Cell. Infect. Microbiol. *9*, 158.

Haenssler, E., Ramabhadran, V., Murphy, C.S., Heidtman, M.I., and Isberg, R.R. (2015). Endoplasmic Reticulum Tubule Protein Reticulon 4 Associates with the Legionella pneumophila Vacuole and with Translocated Substrate Ceg9. Infect. Immun. *83*, 3479–3489.

Haidet, J., Cifarelli, V., Trucco, M., and Luppi, P. (2012). C-peptide reduces pro-inflammatory cytokine secretion in LPS-stimulated U937 monocytes in condition of hyperglycemia. Inflamm. Res. *61*, 27–35.

Harb, O.S., Gao, L.-Y., and Abu Kwaik, Y. (2000). From protozoa to mammalian cells: a new paradigm in the life cycle of intracellular bacterial pathogens. Environ. Microbiol. *2*, 251–265.

Herrmann, V., Eidner, A., Rydzewski, K., Blädel, I., Jules, M., Buchrieser, C., Eisenreich, W., and Heuner, K. (2011). GamA is a eukaryotic-like glucoamylase responsible for glycogen- and starch-degrading activity of Legionella pneumophila. Int. J. Med. Microbiol. *301*, 133–139.

Hielpos, M.S., Fernández, A.G., Falivene, J., Alonso Paiva, I.M., Muñoz González, F., Ferrero, M.C., Campos, P.C., Vieira, A.T., Oliveira, S.C., and Baldi, P.C. (2018). IL-1R and Inflammasomes Mediate Early Pulmonary Protective Mechanisms in Respiratory *Brucella Abortus* Infection. Front. Cell. Infect. Microbiol. *8*, 391.

Horwitz, M.A. (1983a). Formation of a novel phagosome by the Legionnaires' disease bacterium (*Legionella pneumophila*) in human monocytes. J. Exp. Med. *158*, 1319–1331.

Horwitz, M.A. (1983b). The Legionnaires' disease bacterium (*Legionella pneumophila*) inhibits phagosome-lysosome fusion in human monocytes. J. Exp. Med. *158*, 2108–2126.

Horwitz, M.A., and Silverstein, S.C. (1980). Legionnaires' disease bacterium (*Legionella pneumophila*) multiples intracellularly in human monocytes. J. Clin. Invest. *66*, 441–450.

Isberg, R.R., O'Connor, T.J., and Heidtman, M. (2009). The Legionella pneumophila replication vacuole: making a cosy niche inside host cells. Nat. Rev. Microbiol. *7*, 13–24.

Ivanov, S.S., and Roy, C.R. (2013). Pathogen signatures activate a ubiquitination pathway that modulates the function of the metabolic checkpoint kinase mTOR. Nat. Immunol. *14*, 1219–1228.

Jha, A.K., Huang, S.C., Sergushichev, A., Lampropoulou, V., Ivanova, Y., Loginicheva, E., Chmielewski, K., Stewart, K.M., Ashall, J., Everts, B., et al. (2015). Network integration of parallel metabolic and transcriptional data reveals metabolic modules that regulate macrophage polarization. Immunity *42*, 419–430.

Jones, S.C., Price, C.T., Santic, M., and Abu Kwaik, Y. (2015). Selective requirement of the shikimate pathway of Legionella pneumophila for intravacuolar growth within human macrophages but not within Acanthamoeba. Infect. Immun. *83*, 2487–2495.

Kagan, J.C., and Roy, C.R. (2002). Legionella phagosomes intercept vesicular traffic from endoplasmic reticulum exit sites. Nat. Cell Biol. *4*, 945–954.

Kilvington, S., and Price, J. (1990). Survival of *Legionella pneumophila* within cysts of *Acanthamoeba polyphaga* following chlorine exposure. J. Appl. Bacteriol. *68*, 519–525.

Kotewicz, K.M., Ramabhadran, V., Sjoblom, N., Vogel, J.P., Haenssler, E., Zhang, M., Behringer, J., Scheck, R.A., and Isberg, R.R. (2017). A Single Legionella Effector Catalyzes a Multistep Ubiquitination Pathway to Rearrange Tubular Endoplasmic Reticulum for Replication. Cell Host Microbe *21*, 169–181.

Kraakman, M.J., Murphy, A.J., Jandeleit-Dahm, K., and Kammoun, H.L. (2014). Macrophage polarization in obesity and type 2 diabetes: weighing down our understanding of macrophage function? Front. Immunol. *5*, 470.

Labonte, A.C., Tosello-Trampont, A.C., and Hahn, Y.S. (2014). The role of macrophage polarization in infectious and inflammatory diseases. Mol. Cells *37*, 275–285.

Lenartic, M., Jelencic, V., Zafirova, B., Ozanic, M., Marecic, V., Jurkovic, S., Sexl, V., Santic, M., Wensveen, F.M., and Polic, B. (2017). NKG2D Promotes B1a Cell Development and Protection against Bacterial Infection. J. Immunol *198*, 1531–1542.

Lifshitz, Z., Burstein, D., Peeri, M., Zusman, T., Schwartz, K., Shuman, H.A., Pupko, T., and Segal, G. (2013). Computational modeling and experimental validation of the Legionella and Coxiella virulence-related type-IVB secretion signal. Proc. Natl. Acad. Sci. USA *110*, E707–E715.

Lorenzo-Morales, J., Kliescikova, J., Martinez-Carretero, E., De Pablos, L.M., Profotova, B., Nohynkova, E., Osuna, A., and Valladares, B. (2008). Glycogen phosphorylase in Acanthamoeba spp.: determining the role of the enzyme during the encystment process using RNA interference. Eukaryot. Cell *7*, 509–517.

Luo, Z.Q. (2011). Legionella secreted effectors and innate immune responses. Cell. Microbiol. *14*, 19–27.

Marion, C., Limoli, D.H., Bobulsky, G.S., Abraham, J.L., Burnaugh, A.M., and King, S.J. (2009). Identification of a pneumococcal glycosidase that modifies O-linked glycans. Infect. Immun. *77*, 1389–1396.

Mills, E.L., Kelly, B., Logan, A., Costa, A.S., Varma, M., Bryant, C.E., Tourlomousis, P., Dabritz, J.H., Gottlieb, E., Latorre, I., et al. (2016). Succinate Dehydrogenase Supports Metabolic Repurposing of Mitochondria to Drive Inflammatory Macrophages. Cell *167*, 457–470e.13.

Molmeret, M., Horn, M., Wagner, M., Santic, M., and Abu Kwaik, Y. (2005). Amoebae as training grounds for intracellular bacterial pathogens. Appl. Environ. Microbiol. *71*, 20–28.

Moon, E.K., Hong, Y., Chung, D.I., Goo, Y.K., and Kong, H.H. (2014). Down-regulation of cellulose synthase inhibits the formation of endocysts in Acanthamoeba. Korean J. Parasitol. *52*, 131–135.

Mori, M., Mode, R., and Pieters, J. (2018). From Phagocytes to Immune Defense: Roles for Coronin Proteins in *Dictyostelium* and Mammalian Immunity. Front. Cell. Infect. Microbiol. *8*, 77.

Muraille, E., Leo, O., and Moser, M. (2014). TH1/TH2 paradigm extended: macrophage polarization as an unappreciated pathogen-driven escape mechanism? Front. Immunol. *5*, 603.

Murray, H.W., Szuro-Sudol, A., Wellner, D., Oca, M.J., Granger, A.M., Libby, D.M., Rothermel, C.D., and Rubin, B.Y. (1989). Role of tryptophan degradation in respiratory burst-independent antimicrobial activity of gamma interferon-stimulated human macrophages. Infect. Immun. *57*, 845–849.

Nakamura-Tsuruta, S., Yasuda, M., Nakamura, T., Shinoda, E., Furuyashiki, T., Kakutani, R., Takata, H., Kato, Y., and Ashida, H. (2012). Comparative analysis of carbohydrate-binding specificities of two anti-glycogen monoclonal antibodies using ELISA and surface plasmon resonance. Carbohydr. Res. *350*, 49–54.

Oliva, G., Sahr, T., and Buchrieser, C. (2018). The Life Cycle of *L. pneumophila*: Cellular Differentiation Is Linked to Virulence and Metabolism. Front. Cell. Infect. Microbiol. *8*, 3.

Pan, Y., Wang, Y., Cai, L., Cai, Y., Hu, J., Yu, C., Li, J., Feng, Z., Yang, S., Li, X., and Liang, G. (2012). Inhibition of high glucose-induced inflammatory response and macrophage infiltration by a novel curcumin derivative prevents renal injury in diabetic rats. Br. J. Pharmacol. *166*, 1169–1182.

Park, J.M., Ghosh, S., and O'Connor, T.J. (2020). Combinatorial selection in amoebal hosts drives the evolution of the human pathogen Legionella pneumophila. Nat. Microbiol. https://doi.org/10.1038/s41564-019-0663-7.

Pathak, S.K., Basu, S., Basu, K.K., Banerjee, A., Pathak, S., Bhattacharyya, A., Kaisho, T., Kundu, M., and Basu, J. (2007). Direct extracellular interaction between the early secreted antigen ESAT-6 of Mycobacterium tuberculosis and TLR2 inhibits TLR signaling in macrophages. Nat. Immunol. *8*, 610–618.

Price, C.T.D., and Abu Kwaik, Y. (2014). The transcriptome of Legionella pneumophila-infected human monocyte-derived macrophages. PLoS ONE *9*, e114914.

Price, C.T., and Abu Kwaik, Y. (2010). Exploitation of Host Polyubiquitination Machinery through Molecular Mimicry by Eukaryotic-Like Bacterial F-Box Effectors. Front. Microbiol. *1*, 122.

Price, J.V., and Vance, R.E. (2014). The macrophage paradox. Immunity *41*, 685–693.

Price, C.T., Al-Khodor, S., Al-Quadan, T., Santic, M., Habyarimana, F., Kalia, A., and Abu Kwaik, Y. (2009). Molecular mimicry by an F-box effector of Legionella pneumophila hijacks a conserved polyubiquitination machinery within macrophages and protozoa. PLoS Pathog. 5, e1000704.

Price, C.T., Al-Quadan, T., Santic, M., Rosenshine, I., and Abu Kwaik, Y. (2011). Host proteasomal degradation generates amino acids essential for intracellular bacterial growth. Science 334, 1553–1557.

Price, J.V., Jiang, K., Galantowicz, A., Freifeld, A., and Vance, R.E. (2018). Legionella pneumophila Is Directly Sensitive to 2-Deoxyglucose-Phosphate via Its UhpC Transporter but Is Indifferent to Shifts in Host Cell Glycolytic Metabolism. J. Bacteriol. 200, https://doi.org/10.1128/JB.00176-18.

Refai, A., Gritli, S., Barbouche, M.-R., and Essafi, M. (2018). Mycobacterium tuberculosis Virulent Factor ESAT-6 Drives Macrophage Differentiation Toward the Pro-inflammatory M1 Phenotype and Subsequently Switches It to the Anti-inflammatory M2 Phenotype. Front. Cell. Infect. Microbiol. 8, 327.

Reinhold, D., Ansorge, S., and Schleicher, E.D. (1996). Elevated glucose levels stimulate transforming growth factor-beta 1 (TGF-beta 1), suppress interleukin IL-2, IL-6 and IL-10 production and DNA synthesis in peripheral blood mononuclear cells. Horm. Metab. Res. 28, 267–270.

Richards, A.M., Von Dwingelo, J.E., Price, C.T., and Abu Kwaik, Y. (2013). Cellular microbiology and molecular ecology of Legionella-amoeba interaction. Virulence 4, 307–314.

Robb, M., Hobbs, J.K., Woodiga, S.A., Shapiro-Ward, S., Suits, M.D., McGregor, N., Brumer, H., Yesilkaya, H., King, S.J., and Boraston, A.B. (2017). Molecular Characterization of N-glycan Degradation and Transport in Streptococcus pneumoniae and Its Contribution to Virulence. PLoS Pathog. 13, e1006090.

Rolando, M., Sanulli, S., Rusniok, C., Gomez-Valero, L., Bertholet, C., Sahr, T., Marguergon, R., and Buchrieser, C. (2013). Legionella pneumophila effector RomA uniquely modifies host chromatin to repress gene expression and promote intracellular bacterial replication. Cell Host Microbe 13, 395–405.

Rossier, O., and Cianciotto, N.P. (2001). Type II protein secretion is a subset of the PilD-dependent processes that facilitate intracellular infection by Legionella pneumophila. Infect. Immun. 69, 2092–2098.

Rossier, O., Starkenburg, S.R., and Cianciotto, N.P. (2004). Legionella pneumophila type II protein secretion promotes virulence in the A/J mouse model of Legionnaires' disease pneumonia. Infect. Immun. 72, 310–321.

Schaap, P., and Schilde, C. (2018). Encystation: the most prevalent and underinvestigated differentiation pathway of eukaryotes. Microbiology 164, 727–739.

Schroeder, G.N. (2018). The Toolbox for Uncovering the Functions of Legionella Dot/Icm Type IVb Secretion System Effectors: Current State and Future Directions. Front. Cell. Infect. Microbiol. 7, 528.

Shen, X., Banga, S., Liu, Y., Xu, L., Gao, P., Shamovsky, I., Nudler, E., and Luo, Z.Q. (2009). Targeting eEF1A by a Legionella pneumophila effector leads to inhibition of protein synthesis and induction of host stress response. Cell. Microbiol. 11, 911–926.

Shuman, H.A., Purcell, M., Segal, G., Hales, L., and Wiater, L.A. (1998). Intracellular multiplication of Legionella pneumophila: human pathogen or accidental tourist? Curr. Top. Microbiol. Immunol. 225, 99–112.

Sica, A., and Mantovani, A. (2012). Macrophage plasticity and polarization: in vivo veritas. J. Clin. Invest. 122, 787–795.

Sory, M.P., and Cornelis, G.R. (1994). Translocation of a hybrid YopE-adenylate cyclase from Yersinia enterocolitica into HeLa cells. Mol. Microbiol. 14, 583–594.

Stone, B.J., and Abu Kwaik, Y. (1999). Natural competence for DNA transformation by Legionella pneumophila and its association with expression of type IV pili. J. Bacteriol. 181, 1395–1402.

Suzuki, H., Hisamatsu, T., Chiba, S., Mori, K., Kitazume, M.T., Shimamura, K., Nakamoto, N., Matsuoka, K., Ebinuma, H., Naganuma, M., and Kanai, T. (2016). Glycolytic pathway affects differentiation of human monocytes to regulatory macrophages. Immunol. Lett. 176, 18–27.

Swart, A.L., Harrison, C.F., Eichinger, L., Steinert, M., and Hilbi, H. (2018). Acanthamoeba and Dictyostelium as Cellular Models for Legionella Infection. Front. Cell. Infect. Microbiol. 8, 61.

Tannahill, G.M., Curtis, A.M., Adamik, J., Palsson-McDermott, E.M., McGettrick, A.F., Goel, G., Frezza, C., Bernard, N.J., Kelly, B., Foley, N.H., et al. (2013). Succinate is an inflammatory signal that induces IL-1β through HIF-1α. Nature 496, 238–242.

Thomas, S.M., Garrity, L.F., Brandt, C.R., Schobert, C.S., Feng, G.S., Taylor, M.W., Carlin, J.M., and Byrne, G.I. (1993). IFN-gamma-mediated antimicrobial response. Indoleamine 2,3-dioxygenase-deficient mutant host cells no longer inhibit intracellular Chlamydia Spp. or Toxoplasma growth. J. Immunol. 150, 5529–5534.

Torres-Castro, I., Arroyo-Camarena, Ú.D., Martínez-Reyes, C.P., Gómez-Arauz, A.Y., Dueñas-Andrade, Y., Hernández-Ruiz, J., Béjar, Y.L., Zaga-Clavellina, V., Morales-Montor, J., Terrazas, L.I., et al. (2016). Human monocytes and macrophages undergo M1-type inflammatory polarization in response to high levels of glucose. Immunol. Lett. 176, 81–89.

Wang, N., Liang, H., and Zen, K. (2014a). Molecular mechanisms that influence the macrophage m1-m2 polarization balance. Front. Immunol. 5, 614.

Wang, X.F., Wang, H.S., Wang, H., Zhang, F., Wang, K.F., Guo, Q., Zhang, G., Cai, S.H., and Du, J. (2014b). The role of indoleamine 2,3-dioxygenase (IDO) in immune tolerance: focus on macrophage polarization of THP-1 cells. Cell. Immunol. 289, 42–48.

Wynn, T.A., Chawla, A., and Pollard, J.W. (2013). Macrophage biology in development, homeostasis and disease. Nature 496, 445–455.

Yang, X., Pan, Y., Xu, X., Tong, T., Yu, S., Zhao, Y., Lin, L., Liu, J., Zhang, D., and Li, C. (2018). Sialidase Deficiency in Porphyromonas gingivalis Increases IL-12 Secretion in Stimulated Macrophages Through Regulation of CR3, lncRNA GAS5 and miR-21. Front. Cell. Infect. Microbiol. 8, 100.

Yuan, C.H., Zhang, S., Xiang, F., Gong, H., Wang, Q., Chen, Y., and Luo, W. (2019). Secreted Rv1768 From RD14 of Mycobacterium tuberculosis Activates Macrophages and Induces a Strong IFN-γ-Releasing of CD4+ T Cells. Front. Cell. Infect. Microbiol. 9, 341.

Zhu, W., Banga, S., Tan, Y., Zheng, C., Stephenson, R., Gately, J., and Luo, Z.Q. (2011). Comprehensive identification of protein substrates of the Dot/Icm type IV transporter of Legionella pneumophila. PLoS ONE 6, e17638.

Zhu, L., Zhao, Q., Yang, T., Ding, W., and Zhao, Y. (2015). Cellular metabolism and macrophage functional polarization. Int. Rev. Immunol. 34, 82–100.

STAR★METHODS

KEY RESOURCES TABLE

REAGENT or RESOURCE	SOURCE	IDENTIFIER
Antibodies		
Rabbit anti-legionella antiserum	This study	N/A
Mouse anti-glycogen ESG1A9mAB	(Nakamura-Tsuruta et al., 2012)	Gift
Alexa Fluor 488 anti-rabbit IgG	Invitrogen	Cat # A-21206 RRID: AB_141708
Alexa Fluor 555 anti-mouse IgG	Invitrogen	Cat # A-31570 RRID: AB_2536180
Alexa Fluor 594 anti-mouse IgM	Invitrogen	Cat # A-21044 RRID: AB_141424
Alexa Fluor 647 anti-goat IgG	Invitrogen	Cat # A-21447 RRID: AB_141844
Anti-human TNF-α clone MAb1	Biolegend	Cat # 502803 RRID: AB_315251
Anti-human IL-12/23 p40 clone C8.6	Biolegend	Cat # 508803 RRID: AB_315530
Anti-human IFN-γ clone B27	Biolegend	Cat # 506512 RRID: AB_315445
Anti-human IL-4 clone 11B11	Biolegend	Cat # 504121 RRID: AB_11149679
Anti-mouse IDO clone 10.1	Millipore	Cat # 05-840 RRID: AB_310044
Anti-mouse IgG HRP	Thermo Scientific	Cat # 31430 RRID: AB_228307
Anti-rabbit IgG HRP	Thermo Scientific	Cat # 31460 RRID: AB_228341
Anti-β-actin	Proteintech	Cat # 20536-1-AP RRID: AB_10700003
Anti-LAMP2	Novus	Cat # NBP2-22217 RRID: AB_2722697
Anti-KDEL	Abcam	Cat # ab12223 RRID: AB_298945
Bacterial and Virus Strains		
Legionella pneumophila AA100/130b (ATCC BAA-74)	ATCC	Cat # ATCC BAA-74
Escherichia coli BL21	Invitrogen	Cat# C600003
Chemicals, Peptides, and Recombinant Proteins		
EDTA-free protease inhibitors	Pierce	Cat # A32965
LPS	Sigma	L4130
Human IFN-γ	Biolegend	Cat # 570202
Human IL-4	Biolegend	Cat # 574002
Human TNF-α	Biolegend	Cat # 570102
Human IL-12p70	Biolegend	Cat # 573002
M-Per Mammalian Protein Extraction Reagent	Thermo Scientific	Cat # 78505
Koningic acid	Cayman Chemical	Cat # 14079
BAY876	Sigma	Cat # SML1774
1-methyl-D-tryptophan	Cayman Chemical	Cat # 16456
CM-H2DCFDA	Invitrogen	Cat # C6827
Calcofluor white	Sigma	Cat # 18909
Fluorescent Brightener 28	Sigma	Cat # F3543
Phorbol 12-myristate 13-acetate	Sigma	Cat # P1585

(*Continued on next page*)

Continued		
REAGENT or RESOURCE	SOURCE	IDENTIFIER
Critical Commercial Assays		
Direct cAMP ELISA kit	Enzo	Cat # ADI-900-066
Amylase Activity Assay Kit	Sigma	Cat # MAK-009-1KT
EnzyChrom Glycogen assay kit	Bioassay Systems	Cat # E2GN-100
Deproteinizing Sample Preparation Kit	Biovision	Cat # K808-200
High Sensitivity Glucose-6-Phosphate Assay Kit	Sigma	Cat # MAK021-1KT
Glucose Uptake-Glo Assay	Promega	Cat # J1341
Lactate Assay Kit	Sigma	Cat # MAK064-1KT
Tryptophan Assay Kit	Sigma	Cat # MAK254-1KT
Milliplex Assay (Custom setup)	Millipore	Custom order
Mouse Inflammation (8-plex) Panel	Antigenix	MMX270
Human Inflammatory Cytokines Multi-Analyte ELISArray	QIAGEN	Cat # MEH-004A
SuperSignal West Femto Maximum Sensitivity Substrate	Thermo Scientific	Cat # 34095
Experimental Models: Cell Lines		
Human monocyte-derived macrophages from healthy donors	This study	
Acanthamoeba polyphaga	ATCC	Cat # 30461
Experimental Models: Organisms/Strains		
Mouse: A/J		Jackson Laboratories
Oligonucleotides		
lamA flanking DNA F ggatccATAAGCATAAATTTGTTTG	This study	N/A
lamA flanking DNA R cggccgTTGAGTAAATCAGAGAA	This study	N/A
lamA 5′ inverse ctcagttttgtagtgtaataatttttatg	This study	N/A
lamA 3′ inverse agacctttcgatgcaatcaggttaattgcagct	This study	N/A
Kan F /5Phos/CTGTCTCTTATACACATCTCAA	This study	N/A
lamA screening F cagttttgtagtgtaataatttttatgg	This study	N/A
lamA screening R caattaacctgattgcatcgaaa	This study	N/A
lamA screening R caattaacctgattgcatcgaaa	This study	N/A
lamA F, ctcgagtttgtctttttaacgatataataac	This study	N/A
lamA R, ggatccCTAATGCGAGATTGTATTTC	This study	N/A
pGEX lamA F GGATCCATGACAGATTCTATGGGA	This study	N/A
pGEX lamA R GTCGACCTAATGCGAGATTGTATTTC	This study	N/A
lamA D1 F /5Phos/AGCGACTCGAACACCATC	This study	N/A
lamA D1 R /5Phos/GCTGTAGGTTATGTACATC	This study	N/A
lamA E1 F /5Phos/TGCATCAAGGATAACCGG	This study	N/A
lamA E1 R /5Phos/GCTTTATTTAGTAAACGA	This study	N/A
lamA D2 F /5Phos/GGCATGATTCCCACAAAA	This study	N/A
lamA D2 R, /5Phos/TATCGTTCATTGGCGATG	This study	N/A
Recombinant DNA		
pBCSK+*lamA*KO1	This study	N/A
pBCSK+*lamA*KO2	This study	N/A
pBCSK+*lamA*KO3	This study	N/A
pBCSK+*lamA*/C	This study	N/A
pBCSK+*lamA*/C^{D199A}	This study	N/A
pBCSK+*lamA*/C^{E233A}	This study	N/A
pBCSK+*lamA*/C^{D313A}	This study	N/A
pGEX-6p-1-*lamA*^{D199A}	This study	N/A
pGEX-6p-1-*lamA*^{E233A}	This study	N/A
pGEX-6p-1-*lamA*^{D313A}	This study	N/A

Continued

REAGENT or RESOURCE	SOURCE	IDENTIFIER
pCYA-*lamA*	This study	N/A
pON.mCherry	(Gebhardt et al., 2017)	Gift
Software and Algorithms		
Bio-plex Manager 6.0	Bio-rad	Cat # 171STND01
GraphPad Prism 5.01	GraphPad	N/A

LEAD CONTACT AND MATERIALS AVAILABILITY

Further information and requests for reagents may be directed to, and will be fulfilled by the Lead Contact, Yousef Abu Kwaik (abukwaik@louisville.edu). All unique/stable reagents generated in this study are available from the Lead Contact without restriction.

EXPERIMENTAL MODEL AND SUBJECT DETAILS

Isolation of Human Monocyte-Derived Macrophages

Human monocyte-derived macrophages (hMDMs) were isolated from immunocompetent male and female healthy donors who were not involved in previous procedures and test naive. hMDMs were cultured in RPMI 1640 (Corning Cellgro) as described previously (Al-Khodor et al., 2008; Price et al., 2009). To generate hMDMs, total white blood cells were isolated from whole blood taken from healthy donors using a Ficoll-Hypaque gradient. The collected white blood cells were re-suspended in RPMI containing 20% FBS and incubated in 6-well low adherence plates for three days. Adherent cells were then collected and plated into appropriate wells for the experiment in RPMI containing 10% FBS for 2 days. The media was then changed to RPMI containing 5% FBS for one day, and then RPMI containing 1% FBS for one more day, after which hMDMs were ready for experiments. HEK293T cells were cultured in DMEM (GIBCO) supplemented with 10% fetal bovine serum as previously described (Al-Khodor et al., 2008; Price et al., 2009). All methods were carried out and approved in accordance to the University of Louisville Institutional Review Board guidelines and blood donors gave informed consent as required by the University of Louisville Institutional Review Board (IRB # 04.0358).

A/J Mouse Model

For testing the virulence of the Δ*lamA* mutant, specific pathogen free, 6-8 weeks old female A/J mice were used as described previously (Price and Abu Kwaik, 2010; Price et al., 2009). All mice were maintained as breeding colonies under specific pathogen-free conditions at the Animal Facility, Faculty of Medicine, University of Rijeka . Experiments were approved by the Ethical Committee of the School of Medicine and conducted in accordance with the international guidelines for animal care and experimental use. Groups of 3 A/J mice were infected intratracheally with 1×10^6 CFUs. At 2, 12, 24, 48 and 72 h after infection mice were humanely sacrificed and lungs, liver and spleen were harvested and homogenized in 5 mL of sterile saline followed by cell lysis in distilled water.

Microbial Strains

L. pneumophila strain AA100/130b (ATCC BAA-74), the T2SS-deficient mutant (Δ*lspG*), Δ*ankB* and Δ*dotA* T4SS-deficient mutant (Δ*T4SS*) were grown on BCYE agar or BYE broth media at 37°C with antibiotic selection as appropriate. *E. coli* BL21 was grown on LB agar or broth at 37°C with antibiotic selection as appropriate.

METHOD DETAILS

Generation of a *lamA* Knockout Mutant

To generate an isogenic Δ*lamA* deletion mutant, 2 kb of DNA flanking either side of the *lamA* gene was amplified using PCR using primers listed in the Key Resources Table and cloned into the shuttle vector, pBCSK+, resulting in pBCSK+*lamA*KO1. To delete the entire *lamA* gene within pBCSK-*lamA*KO1, inverse PCR was employed using primers listed in the Key Resources Table resulting in a pBCSK+*lamA*KO2. The kanamycin resistance cassette from the Ez-Tn5 transposon was amplified using primers listed in the Key Resources Table and the resulting PCR product was subcloned into pBCSK+*lamA*KO2 in between the *lamA* flanking DNA regions using standard molecular biology procedures, resulting in pBCSK+*lamA*KO3. This plasmid was introduced into *L. pneumophila* AA100 via natural transformation, as described previously (Stone and Abu Kwaik, 1999). Following 3 days, natural transformants were recovered by plating on BCYE agar supplemented with 50 μg/mL kanamycin. To confirm deletion of the *lamA* gene in the transformants, PCR was used using the primers listed in the Key Resources Table. To complement the *lamA* mutant, PCR was used to amplify the *lamA* gene and its upstream promoter region using primers listed in the Key Resources Table, and subcloned into pBCSK+, generating pBCSK+*lamA/C*. This plasmid was introduced into the *lamA* mutant via electroporation as described previously (Chen et al., 2006). Complemented *lamA* mutants were selected on BCYE plates supplemented with 5 μg/mL chloramphenicol, resulting in the complemented strain, *lamA/C*. For infections of cell monolayers, *L. pneumophila* was grown in BYE broth media with appropriate antibiotic selection at 37°C with shaking to post-exponential phase (OD550nm 2.1-2.2).

Translocation Assay

To assess translocation of LamA by *L. pneumophila* during infection of host cells, an adenylate cyclase fusion to the N terminus of LamA (Sory and Cornelis, 1994) was generated using standard molecular biology techniques. A total of 1 X 10⁶ hMDMs were infected with wild type or ΔT4SS mutant *L. pneumophila* harboring plasmids expressing various adenylate cyclase fusions at an MOI of 20 for 1 h as described previously (Price et al., 2009; Sory and Cornelis, 1994). Following infection, the cell monolayers were lysed and processed to assess cAMP concentration by ELISA using the Direct cAMP ELISA kit (Enzo) according to the manufacturer's instructions.

Amylase Activity Assay

To determine if LamA exhibits amylase activity, the *lamA* gene was cloned into the IPTG-inducible GST-fusion expression vector pGEX-6p-1 (Amersham) and expressed in *E. coli* BL21 using primers listed in the Key Resources Table. Additionally, residues constituting the predicted catalytic pocket were substituted to alanine's using inverse PCR using primers listed in the Key Resources Table. *E. coli* cultures (5 ml) harboring either the empty vector or *lamA* and the various catalytic inactive mutants were grown in LB media at 37°C with shaking until the OD600 reached 0.7. The cultures were split and one half was induced with 0.1 mM IPTG for 2.5 h at room temperature. One ml of each culture was pelleted by centrifugation and the cells were lysed in 0.5 mL lysis buffer (0.1% v/v Triton X-100, 10 mM Tris pH7.5, 150 mM NaCl), containing protease inhibitors (Pierce EDTA-Free Protease Inhibitors). Insoluble material was pelleted by centrifugation (16000 x g, 10 min, 4°C) and the resulting supernatant was retained. Expression of fusion proteins was similar in all cultures (Figure S1B). To measure amylase activity, 25 μl of supernatant was analyzed using an Amylase Assay Kit (Sigma), following the manufacturer's instructions.

Analysis of Intracellular Glycogen

Glycogen levels in hMDMs during infection by *L. pneumophila* were determined using the EnzyChrom Glycogen assay kit (Bioassay Systems). Briefly, a total of 3 X 10⁶ hMDMs were seeded into 6 well plates and infected with the wild type, ΔT4SS, ΔlamA, lamA/C and the catalytically inactive mutants at an MOI of 10 for 1 h and 6 h. As a control for glycogenolysis, hMDMs were starved of glucose 1 h prior to the commencement of the experiment. Cells were harvested and lysed in 25 mM sodium citrate containing 60 mM NaF. Following centrifugation at 13000 X g for 5 min to pellet cellular debris, the supernatants were then analyzed following the manufacturers' instructions. Degradation of intracellular glycogen was also determined using confocal microscopy. To achieve this, hMDMs were plated into 24-well plates containing glass coverslips (2 × 10⁵ cells per well) and infected with either post-exponential phase wild type, ΔT4SS, ΔlamA and lamA/C, and a type II secretion defective mutant (ΔlspG) bacteria at an MOI of 1. At various time points, the monolayers were fixed and permeabilized using methanol at −20°C for 5 min. The monolayers were labeled with rabbit anti-*Legionella* antiserum (1/1000 dilution), mouse anti-glycogen antibody (ESG1A9mAB, 1/50 dilution) (Nakamura-Tsuruta et al., 2012), a kind gift from Dr Ashida (Kobe University) and counter-labeled with Alexa Fluor 488 anti-rabbit IgG antibody and Alexa Fluor 594 anti-mouse IgM (1/4000 dilution, Invitrogen) and DAPI to stain nuclei. The cells were examined by confocal microscopy using an Olympus FV1000 laser scanning confocal microscope (Olympus). Quantification of glycogen granules was performed manually by counting Z stack images (8 μM depth with 0.2 μM slices) of infected cells. Over 100 infected cells were counted for each condition and performed in triplicate.

Determination of Cytosolic Glucose-6-phosphate

To determine G6P levels in either infected hMDMs or *A. polyphaga* a total of 3 × 10⁶ cells were infected with either wild type, ΔT4SS, ΔlamA or lamA/C bacteria at an MOI of 20 for the time indicated in each experiment. Following infection, the infected cells were collected in ice-cold PBS and rapidly homogenized on ice. Samples were centrifuged (16000 x g for 20 min at 4°C), and the resulting supernatants were subjected to deproteinization using a Deproteinizing Sample Preparation Kit (Biovision) following the manufacturer's instructions. For measuring G6P in amoebae undergoing encystation, amoebae were infected as described above. At 1 h and 4 h post-infection, aliquots of the infected amoebae were lysed and treated as above. The remaining amoebae were washed in Pages saline and the transferred to encystation buffer. At 6 and 12 h post-encystation, amoebae and cysts were collected by centrifugation and lysed by sonication. The samples were analyzed for G6P using a High Sensitivity Glucose-6-Phosphate Assay Kit (Sigma) according to the manufacturer's instructions with a Synergy H1 microplate reader (Biotek).

Glucose Uptake Assay

To measure uptake of glucose by *L. pneumophila* infected hMDMs, the Glucose Uptake-Glo Assay (Promega) was used. Briefly, a total of 1 X 10⁵ hMDMs were seeded into black 96 well plates and infected with wild type, ΔT4SS, ΔlamA or lamA/C bacteria at an MOI of 10 for 1 h or 6 h in triplicate. As a control, hMDMs were pre-stimulated with LPS/IFN-γ for 24 h prior to the assay. At 1 h or 6 h post-infection, the culture media was removed and PBS containing 1mM 2-deoxyglucose was added for 10 min. Glucose uptake was blocked by adding 0.2 μM BAY876 (Sigma) prior to the assay. Glucose uptake was then directly measured according to the manufacturer's instructions with a Synergy H1 microplate reader (Biotek).

In Vitro Broth Culture Growth Curves

To determine growth of the ΔlamA mutant during *in vitro* broth culture relative to the wild type strain, cultures of both the wild type and ΔlamA mutant were grown in BYE medium at 37°C to an OD550 of ∼1. The cultures were diluted to an OD550 of 0.05 in triplicate with

fresh BYE media and incubated at 37°C with shaking at 200 rpm for a further 24 h, during which the optical density was measured periodically. Additionally, to determine if glucose impacts growth of the wild type strain, growth curves were performed as described above with BYE supplemented with increasing concentrations of glucose, up to 44 mM.

Intracellular Replication

The wild type strain and the isogenic mutants, ΔT4SS and ΔlamA, and lamA/C and catalytically inactive mutants were grown to post-exponential phase in BYE broth at 37°C prior to infection and used to infect hMDMs, or *A. polyphaga* as described previously (Al-Khodor et al., 2008; Price et al., 2009). A total of 1 X 10^5 host cells per well were plated in 96 well plates and infected with *L. pneumophila* at an MOI of 10 for 1 h and then treated for 1 h with gentamicin to kill remaining extracellular bacteria as previously described (Al-Khodor et al., 2008; Price et al., 2009). Over a 24-48 h time course, the host cells were lysed with sterile water (hMDMs), or 0.02% v/v Triton X-100 (*A. polyphaga*) and *L. pneumophila* CFUs were determined by plating serial dilutions onto BCYE agar.

To analyze replicative vacuoles, 2 X 10^5 hMDMs were seeded onto glass coverslips in 24-well plates. The cell monolayers were infected with wild type, ΔT4SS, ΔlamA, or lamA/C at an MOI of 10 for 1 h and then the monolayers were treated with gentamicin for 1 h to kill remaining extracellular bacteria as previously described (Al-Khodor et al., 2008; Price et al., 2009). Following extensive washing to remove gentamicin, the infection proceeded for 6 and 8 h. At 6 and 8 h the monolayers were permeabilized and fixed at −20°C in 100% methanol for 5 min, and then labeled with rabbit anti-*Legionella* antiserum (1/1000 dilution) and counter-labeled with Alexa Fluor 488 anti-rabbit antibody (1/4000 dilution, Invitrogen) and DAPI to stain the nuclei. Monolayers were examined by confocal microscopy. A total of 100 replicative vacuoles from 100 individual cells were analyzed for each experimental condition and performed in triplicate.

For culture supernatant transfer experiments, hMDMs were infected as above for analysis of replicative vacuoles or stimulated with 100ng LPS and 10U IFNγ for 8 h. Culture supernatants were collected and filter-sterilized through 0.22μM syringe filters and used as culture media for infection of fresh hMDMs with the ΔlamA mutant as described above. Cytokines were neutralized for 1 h prior to infection using anti-IFNγ, anti-IL12, anti-TNFα or anti-IL4 (1/100 dilution) (Biolegend). Analysis of replicative vacuoles was performed as described above. To determine the impact of glycolysis on *L. pneumophila* replication, hMDMs were pretreated with 1 mM NaF or koningic acid for 1 h prior to infection with the wild type or ΔlamA mutant strain as described above for 8 h. The inhibitors were maintained throughout the experiment and analysis of replicative vacuoles was performed as described above. For tryptophan supplementation experiments, the RPMI media was supplemented with an additional 90 or 180 μM tryptophan prior to infection of hMDMs with the wild type or ΔlamA mutant strain as described above for 8 h. The additional tryptophan was maintained throughout the experiment and analysis of replicative vacuoles was performed as described above.

Co-infection of hMDMs with Wild Type and lamA Bacteria

To determine the impact of co-infection on intracellular replication of wild type and ΔlamA mutant bacteria, the wild type strain was transformed with pON.mCherry (Gebhardt et al., 2017), resulting in constitutive expression of mCherry fluorescent protein. hMDMs were infected with the wild type pON.mCherry and ΔlamA mutant bacteria alone or in combination (MOI 5) as described for replicative vacuole analysis. At 8 h post-infection, hMDM monolayers were fixed using 3.7% v/v formaldehyde for 15 min and then permeabilized with 0.1% v/v Triton X-100 for 15 min. The monolayers were labeled with anti-*Legionella* antiserum as described above. Analysis of replicative vacuoles was performed as described above.

Determination of Secreted Lactate by Infected hMDMs

To determine lactate secretion by infected hMDMs into the culture medium, a total of 1 × 10^6 hMDMs in triplicate were infected with either wild type, ΔT4SS, ΔlamA or lamA/C bacteria at an MOI of 10 for 6 h. Following infection, the culture media was retained and cooled on ice and subjected to deproteinization using a Deproteinizing Sample Preparation Kit (Biovision) following the manufacturer's instructions. The samples were analyzed for lactate using a Lactate Assay Kit (Sigma) according to the manufacturer's instructions with a Synergy H1 microplate reader (Biotek).

Analysis of Indoleamine 2,3-dioxygenase

To determine if indoleamine 2,3-dioxygenase 1 (IDO1) expression by hMDMs was altered by infection by *L. pneumophila*, a total of 3 × 10^6 hMDMs were infected with the wild type, ΔT4SS, ΔlamA or lamA/C bacteria at an MOI of 10 for 2 and 4 h. Following infection, the monolayers were lysed using M-PER reagent (Thermo) containing protease inhibitors (Pierce). Samples were electrophoresed by SDS-PAGE and transferred to PVDF membranes for western blotting using standard techniques. To detect IDO, mouse anti-IDO antibody clone 10.1 (Millipore) was used at 1/100 dilution and detected with an anti-mouse HRP conjugate (Pierce). For chemiluminescence, SuperSignal West Femto (Thermo) was used according to the manufacturer's instructions, and imaged using a C300 imager (Azure Biosystems). Membranes were stripped using standard techniques are re-probed using a rabbit anti-β-actin antibody to serve as a loading control.

To determine the cytosolic concentration of tryptophan in hMDMs infected with *L. pneumophila* the Tryptophan Assay Kit (Biovision) was used. Briefly, a total of 3 X 10^6 hMDMs were infected with wild type, ΔT4SS, ΔlamA, lamA/C, the catalytically inactive mutant or formalin killed wild type bacteria at an MOI of 20, for 4 h in triplicate. As a control, 1μM 1-methyl-D-tryptophan was added to wild type infected wells 1 h prior to commencement of the experiment to block IDO1 activity. Cells were harvested and analyzed according to the manufacturers' instructions.

To determine the impact of IDO1 on *L. pneumophila* replication, hMDMs were treated with 0.5, 1 or 2μM 1-methyl-D-tryptophan 1 h prior to infection. Following this treatment, hMDMs were infected with the wild type or Δ*lamA* mutant bacteria for 6 h and the inhibitor was maintained throughout the experiment. Following infection, analysis of replicative vacuoles was performed as described above.

Analysis of Reactive Oxygen Species Production and Intracellular Trafficking of *L. pneumophila*

Production of reactive oxygen species by infected hMDMs was performed using the indicator dye, CM-H2DCFDA (Invitrogen). A total of 1×10^5 hMDMs were seeded into 96-well plates and infected with the wild type, Δ*T4SS*, Δ*lamA* or formalin-killed wild type bacteria at an MOI of 20. As a positive control, hMDMs were stimulated with phorbol 12-myristate 13-acetate (100 ng/mL). CM-H2DCFDA was added to the wells at a final concentration of 2μM and the cells were placed into a Synergy H1 microplate reader (Biotek) set at 37°C. Fluorescence detection was performed using Ex492nm and Em518nm every 2 min for a total of 50 min.

To determine if the Δ*lamA* mutant exhibits similar intracellular trafficking and LCV development as the wild type strain, hMDMs were infected at MOI of 10 for 2 h. The hMDMs were fixed and permeabilized with −20°C methanol for 5 min and labeled with rabbit anti-*L. pneumophila* antiserum (1/1000 dilution) and mouse anti-LAMP2 (lysosome marker) or KDEL (endoplasmic reticulum marker) (1/2000 and 1/200 dilutions respectively, Transduction Labs, Stressgen). Anti-mouse IgG Alexa Fluor 555 and anti-rabbit IgG Alexa Fluor 488 secondary antibodies (1/4000 dilution, Invitrogen) were used to visualize vacuolar markers and *L. pneumophila* respectively. A total of 100 LCVs from 100 individual cells were analyzed by confocal microscopy for each experimental condition and performed in triplicate.

Cytokine Analysis

To determine cytokine production by hMDMs, a total of 3×10^6 cells per well were plated in 6 well plates and infected with *L. pneumophila* at an MOI of 20 for 1 h and then treated for 1 h with gentamicin to kill remaining extracellular bacteria. Culture supernatants were collected 6 h post-infection and then analyzed using the Milliplex (Millipore) assay. Assays were performed according to the manufacturer's instruction. Standards or culture supernatant samples were mixed with antibody-bound magnetic beads, and incubated overnight at 4 °C. Beads were washed and then incubated with the biotinylated detection antibody for one h at room temperature. The beads were incubated with phycoerythrin-labeled streptavidin for thirty minutes at room temperature and the median fluorescent intensities were quantified with a Bio-plex 200 analyzer and analyzed with Bio-plex Manager 6.0 software. All samples were measured in duplicate. In some experiments 1mM NaF was added to block glycolysis 1 h prior to infection and maintained throughout the experiment. Following, 6 h infection, culture supernatants were retained and immediately analyzed for cytokines using Human Inflammatory Cytokines Multi-Analyte ELISArray (QIAGEN), following the manufacturer's instructions. Infections were performed in triplicate.

Mouse Model of Infection

For testing the virulence of the Δ*lamA* mutant, specific pathogen free, 6-8 weeks old A/J mice were used as described previously (Price and Abu Kwaik, 2010; Price et al., 2009). Groups of 3 A/J mice were infected intratracheally with 1×10^6 CFUs. At 2, 12, 24, 48 and 72 h after infection mice were humanely sacrificed and lungs, liver and spleen were harvested and homogenized in 5 mL of sterile saline followed by cell lysis in distilled water. To determine CFUs, serial 10-fold dilutions were plated on BCYE agar and incubated at 37°C. For histopathology, lungs of infected mice were fixed in 10% neutral formalin and embedded in paraffin. Serial 5 μm sections were cut, stained with hematoxylin and eosin (H&E), and analyzed by light microscopy. Twenty random high-powered fields (HPFs) were assessed to grade inflammation severity including alveolar and bronchial damage as well as percentage of parenchyma involved. The histology assessment included the number of the mononuclear cells and percent of parenchyma involved by using modification of double-blind scoring method at a magnification of 40x, as described previously (De Simone et al., 2014). The inflammation process was graded normal (score of 0) when there were 0-19 monocular cells infiltrates per HPF with no alveolar and bronchial involvement, mild (score of 1) for 20 to 49 cells per HPF including mild damage of alveolar and bronchial regions, moderate (score of 2) for 50 to 99 cells per HPF with moderate alveolar and bronchial inflammation, or severe (score of 3) for 100 to 200 mononuclear cells per HPF with severe effacement of alveolar and bronchial regions. The murine lung section was examined in sagittal direction and percent of parenchyma involved was scored as 0 when no area was compromised. The involvement of the parenchyma was scored as 1 when up to 25% of the total area was occupied by inflammatory exudate; was scored as 2 when 26 to 50% of parenchyma area was occupied with inflammatory cells, 3 if comprised more than 51%. The total histology score was calculated as an average of individual criteria scores. The uninfected tissue was used as a baseline score.

To determine cytokine production, the broncho-alveolar lavage (BAL) of infected mice was performed at 2, 12, 24, 48 and 72 h after infection. BAL was collected using a 1 mL syringe with 0.5 ml of fresh saline via the trachea. After three lavages, approximately 350 μL of BAL was recovered and stored at −25°C for determination of cytokine levels. The levels of cytokines KC, MCP-1, TNFα, IL6, IL1a, IL4, IL10, IFN-γ and IL12p70 were determined using Antigenix Mouse Inflammation Kit on a BD FACSAria flow cytometer (Lenartic et al., 2017).

Encystation of *Acanthamoeba polyphaga* Infected with *L. pneumophila*

Amoebas were grown to 50%–80% confluence in tissue culture flasks in PYG at 25°C. Prior to infection, the medium was replaced with PY, and adherent amoebas were scraped and harvested, adjusted to 2×10^6 per ml. Six well plates were seeded with 1 mL amoebas, and incubated at 35°C for 30-60 min. Post-exponential *L. pneumophila* cultures were diluted to 1×10^8 per ml in PY,

and 1 mL was added to each well, for a MOI of 50. Plates were centrifuged for 5 min at 200 x g, then incubated at 35°C for 4 h. Mono-layers were washed 1 x with 2 mL of Page's saline (PS), then 3 mL of encystation buffer (0.1M KCl, 0.02M 2-amino-2-methy-1,3-pro-panediol, 0.008M $MgSO_4$, 0.001 $NaHCO_3$, 0.0004M $CaCl_2$, pH 9) was added to each well. Plates were incubated at 35°C for 24, 48, or 72 h. Amoebas were harvested by scraping, centrifuged 5 min at 500 x g, washed 1 x with PS, centrifuged again, and resuspended in 1 mL 5% formaldehyde in PS. Tubes were rotated at room temperature for 1 h, washed 1 x with PS, centrifuged again, and resus-pended in 1 mL blocking buffer, 3% BSA in PBS, and stored at 4°C. After blocking, amoebas were centrifuged, and resuspended in 1 mL blocking buffer containing goat anti-*Legionella* antiserum. Tubes were rotated 1 h at room temp, centrifuged, and pellets were washed 1 x with PBS, and centrifuged again. Pellets were resuspended in blocking buffer containing Alexa Fluor 647 donkey anti-goat (Invitrogen) and 0.01% calcofluor white, Fluorescent Brightener 28 (Sigma). Tubes were rotated for 1 h at room temp, centri-fuged, and pellets were washed 1 x with PBS, and centrifuged again. Pellets were resuspended in 800 μl PBS and stored at 4°C. Flow cytometry was done on a 4 laser, 18 parameter BD LSRFortessa, using the Pacific Blue parameter for detection of calcofluor white. Analyses were done with BD FACSDiva software and Flowing Software 2.5. Samples were also used for confocal microscopy.

QUANTIFICATION AND STATISTICAL ANALYSIS

Statistical parameters including the exact value of n, (mean ± SD) and statistical significance are reported in the Figures and Fig-ure Legends. Statistical analysis was performed in GraphPad PRISM 5.

DATA AND CODE AVAILABILITY

This study did not generate/analyze datasets or code.